energy&fuels

pubs.acs.org/EF Article

Investigation of Island/Single-Core- and Archipelago/Multicore-Enriched Asphaltenes and Their Solubility Fractions by Thermal Analysis Coupled with High-Resolution Fourier Transform Ion Cyclotron Resonance Mass Spectrometry

Anika Neumann, Martha Liliana Chacón-Patiño, Ryan P. Rodgers, Christopher P. Rüger,* and Ralf Zimmermann

Cite This: *Energy Fuels* 2021, 35, 3808−3824 Read Online

ACCESS | Metrics & More | Article Recommendations | Supporting Information

ABSTRACT: Despite extensive research, the molecular-level chemical characterization of asphaltenes, a highly aromatic solubility fraction of petroleum, remains an analytical challenge. This fraction is related to diverse problems in crude oil exploration, transportation, and refining. Two asphaltene architecture motifs are commonly discussed in the literature, "island" (single-core)- and "archipelago" (multicore)-type structures. The thermal desorption and pyrolysis behavior of island- and archipelago-enriched asphaltenes and their extrography fractions was investigated. For this purpose, the evolved chemical pattern was investigated by thermal analysis coupled with ultrahigh-resolution mass spectrometry (Fourier transform ion cyclotron resonance mass spectrometry (FT-ICR MS)). Soft atmospheric pressure chemical ionization preserved the molecular information of the thermal emission profile. Time-/temperature-resolved analysis allowed the chemical characterization of the occluded material as well as of asphaltene building blocks during pyrolysis. Regarding the thermogravimetric information, the island-type enriched sample (Wyoming asphaltenes) revealed a significantly higher coke residue after the pyrolysis process compared to the archipelago-type enriched sample (Athabasca asphaltenes). In contrast to whole asphaltenes, extrographic fractions revealed that occluded material evolved during the desorption phase. For the acetone fraction, this effect was the most abundant and suggests cooperative aggregation, which persists at high temperatures. Pyrolysis revealed a bimodal behavior for most of the compound classes, suggesting the presence of both architecture motifs in each asphaltene. double-bond equivalent (DBE) vs #C diagrams of the pyrolysis molecular profile revealed specific compositional trends: compounds with high DBE values and short alkylation are likely to be originated from island-type asphaltenes, whereas species with low DBE values and high carbon numbers likely derive from archipelago-type asphaltenes. In the asphaltene structural debate, thermal analysis ultrahigh-resolution mass spectrometry serves as an additional technique and supplements results obtained by other techniques, such as direct infusion approaches. Consistent results on the structural motifs are indicated by the molecular fingerprint visualized by DBE vs #C diagrams and serve as a measure for the dominance of a structural motif.

INTRODUCTION

During the production, transportation, and refining of crude oils, asphaltenes are often related to problems such as deposit formation, fouling of catalysts, or destabilization of the crude oil mixture.[1−6] Due to the high economic relevance, asphaltenes are therefore of significant interest in petroleum chemistry. However, because of their high chemical and structural complexity, and despite recent advances in mass spectrometry and atomic force microscopy (AFM),[7−9] asphaltenes remain an analytical challenge.

Asphaltenes are defined as the fraction of crude oil that is soluble in toluene but insoluble in paraffinic solvents such as *n*-pentane (C5), cyclo-/*n*-hexane (C6), and *n*-heptane (C7). They are composed of pericondensed aromatic cores with peripheral alkyl chains (island/single-core structural motif) as well as smaller aromatic cores linked by alkyl or naphthenic bridges (archipelago/multicore structural motif) and contain higher amounts of heteroatoms (sulfur, nitrogen, oxygen) and metals (e.g., vanadium and nickel).[10−12] Due to their high aggregation tendency,[13,14] the molecular weight range of monomeric asphaltenes was debated for decades. Meanwhile, researchers mostly agree on a mass range of 200−1500 Da with an average molecular weight of 500−800 Da.[15−19]

Not only the asphaltenes' molecular weight was a controversial issue in the literature, but also the molecular architecture is still a subject of investigation. The island model was introduced in the early 1960s by Yen et al.[20] and was later modified by Mullins and co-workers.[21] Since then, the island structural motif has been supported by a variety of analytical techniques. For example, atomic force microscopy (AFM) predominantly revealed highly peri- and cata-condensed polycyclic aromatic hydrocarbon (PAH) structures with 4−20 fused rings in one aromatic core,[7,8,22] and archipelago-type

Received: November 6, 2020
Revised: December 14, 2020
Published: December 29, 2020

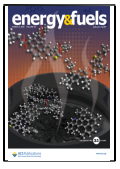

https://dx.doi.org/10.1021/acs.energyfuels.0c03751
Energy Fuels 2021, 35, 3808−3824

asphaltenes were detected too.[23,24] Nuclear magnetic resonance (NMR), however, provides additional evidence for single aromatic cores with four to seven fused rings.[11,25,26] Further, different mass spectrometric techniques with several ionization methods preferentially exhibited island-type asphaltenes. Laser desorption laser ionization mass spectrometry (L^2MS) of asphaltene model compounds revealed significant similarity of island-type species to the fragmentation behavior of real asphaltene samples.[27,28] Similar results were observed for model compounds as well as asphaltenes using mass spectrometry with collision-induced dissociation (CID) fragmentation, which results in an average number of three to eight fused rings with up to 20 carbon atoms in alkyl sidechains.[19,29−31]

Nonetheless, although the island model serves to describe some asphaltene properties, such as reservoir geodynamics, it is incongruent with asphaltene behavior in several scenarios, e.g., products observed after thermal upgrading or pyrolytic degradation. After thermal cracking, the newly formed maltene fraction has been found to consist of alkylated 1−5-ring aromatics, alkanes, and alkenes, as well as naphthenes.[32−37] These observations are supported by Savage et al., who investigated structural building blocks of pyrolyzed asphaltenes with gas chromatography (GC)−MS.[38,39] Furthermore, Strausz and co-workers provided detailed compositional and structural information on asphaltene pyrolysis products by applying gas chromatographic (GC and GC−MS) as well as spectroscopic techniques.[12,36,40,41] Karimi et al.[33] found by thin-film pyrolysis small quantitative differences in building blocks revealed from asphaltenes of different geological origins. Rueda-Velásquez et al.[32] investigated asphaltene building blocks after thermal cracking under hydrogenation conditions. They found small aromatic, alkylated fragments providing evidence for archipelago-type structures, while 35−45% of the samples remained as high-boiling-point, highly aromatic compounds.[32]

In the last two decades, high-resolution Fourier transform ion cyclotron resonance mass spectrometry (FT-ICR MS) contributed valuable insights into the asphaltene compositional space due to its ultrahigh resolving power and mass accuracy. McKenna et al.[43] defined the asphaltene compositional space by direct infusion (DI) atmospheric pressure photoionization (APPI) FT-ICR MS. The authors concluded that asphaltenes are preferentially composed of highly aromatic/alkyl-depleted compounds with double-bond equivalents (DBEs = number of rings and double bonds[42]) of over 20 and abundance-weighted H/C ratios between 0.8 and 0.9.[43] Based on these results, it was concluded that asphaltenes are an extension of the maltene compositional space in aromaticity but share a similar carbon number.[43] Subsequently, Podgorski et al.[44] revealed, by infrared multiphoton dissociation (IRMPD), evidence of the existence of both structural motifs due to the presence of fragment ions with prevalent DBE values below 15 (archipelago fragments) as well as highly aromatic compounds with DBEs of up to 25 (island fragments).[44] Further evidence for the presence of archipelago-type asphaltenes was revealed by analyzing the evolved gas mixture of asphaltenes by thermogravimetry (TG) coupled with FT-ICR MS.[34,45] The authors inferred an average archipelago structure composed of three aromatic cores linked by alkyl bridges for the interlaboratory sample known as PetroPhase-2017 asphaltenes.[45,46] McKenna et al. further concluded the presence of archipelago structures in asphaltenes by observing small thermal fragments during distillation of high petroleum boiling cuts.[10] Recently, the predominance of island-type asphaltenes in DI-FT-ICR MS spectra was found to be caused by efficient ionization, or high monomer ion yield, whereas archipelago-type asphaltenes were revealed to poorly ionize due to a higher aggregation tendency.[47,48] Extrography fractionation of asphaltenes revealed that island and archipelago structural motifs are enriched in different solubility fractions, such as acetone (enriched in species with high monomer ion yield, island-dominant) or tetrahydrofuran/methanol (enriched in species with low monomer ion yield, archipelago-dominant).[49,50] The predominance of both structures depends not only on the regarded fraction but also on the origin of the asphaltenes as well as the investigated molecular mass range.[51] In a recent study, Athabasca bitumen and Wyoming deposit asphaltenes were investigated by APPI-IRMPD-FT-ICR MS. While Athabasca asphaltenes revealed dominant archipelago-like fragmentation throughout the mass range, Wyoming asphaltenes revealed dominant islandlike fragmentation for smaller-molecular-weight asphaltenes, whereas higher m/z values exhibited both structural fragmentation pathways.[51]

In this study, we combine the extrography fractionation of asphaltenes from different geological origins[49,51] with temperature-resolved analysis by TG-FT-ICR MS to investigate asphaltene solubility fractions enriched in archipelago and island structural motifs. As an ionization technique, atmospheric pressure chemical ionization (APCI) was applied, which covers semipolar to polar compounds expected to be present in the solubility fractions. Its value for analyzing complex mixtures in combination with TG-FT-ICR MS has been demonstrated in previous studies.[34,45,52] Here, we showed that TG-FT-ICR MS can address the controversial issue of the predominant structural motif of asphaltenes exhibiting corresponding results to previous studies on the same asphaltenes with DI-IRMPD-FT-ICR MS.[49,51] Both investigated asphaltenes obtained from Athabasca bitumen and Wyoming deposit, separately, revealed differences in the compositional space, the presence of occluded material, and coke formation during evolved gas analysis. Nonetheless, both asphaltenes revealed island- and archipelago-related pyrolysis fragments, whose abundances were found to vary between the geological origin and the different solubility fractions.

MATERIALS AND METHODS

Asphaltene Precipitation from Crude Oils. Asphaltenes were isolated from Athabasca bitumen and Wyoming petroleum deposit following a slightly adapted version of the standard method D6560-12.[46,53] Briefly, petroleum samples were mixed with *n*-heptane in a 1/40 volume ratio under sonication and refluxed heating at 85 °C for 1 h. The mixture of oil/*n*-heptane was allowed to settle overnight, protected from light, and subsequently filtrated (Whatman 2 paper filter) to recover the precipitated solids. Asphaltene cleaning was performed in a Soxhlet apparatus with hot *n*-heptane under a nitrogen atmosphere for 120 h. The cleaned C7 insolubles were recovered by dissolution in hot toluene and dried under nitrogen. Solid asphaltenes were subjected to an additional cleaning step, which consists of four cycles of asphaltene crushing and Soxhlet extraction with *n*-heptane to remove coprecipitated C7 solubles.

Extrography Fractionation. Extrography is a separation method that involves sample adsorption on a polar adsorbent (e.g., SiO_2, alumina, cellulose) and subsequent desorption with specific solvents. In short, asphaltenes were adsorbed on silica gel with a mass loading of 1 wt % (10 mg of asphaltenes/1 g of dried SiO_2); the mixture was dried under nitrogen and then extracted with acetone, *n*-heptane/toluene (Hep/Tol 1:1 v/v), and toluene/tetrahydrofuran/methanol

https://dx.doi.org/10.1021/acs.energyfuels.0c03751
Energy Fuels 2021, 35, 3808−3824

(Tol/THF/MeOH 10:10:1). The fractions were dried under nitrogen and stored in amber-glass vials. It is essential to point out that using a low mass loading (≤1 wt %) and drying the silica gel after acetone extraction are essential conditions to optimize the separation process as shown in the literature.[49]

Thermal Gravimetry Coupled with Atmospheric Pressure Chemical Ionization Fourier Transform Ion Cyclotron Resonance Mass Spectrometry (TG-APCI-FT-ICR MS). Asphaltene samples were investigated by thermal gravimetry (TG) coupled with APCI-FT-ICR MS. A detailed description of the setup can be found elsewhere.[54] For the asphaltenes, approximately 0.3−0.5 mg of the sample material was introduced in an aluminum crucible to the thermobalance (TG 209 cell thermobalance, Netzsch, Selb, Germany) without further sample pretreatment. The samples were then heated under a nitrogen atmosphere with the following temperature program: starting at 20 °C (held for 2 min), heating from 20 to 600 °C at a heating rate of 5 K/min (held for 10 min). The evolved gas mixture was transferred to the ionization chamber of the mass spectrometer via a slight overpressure over a heated transfer line (8 mbar, 300 °C). Positive-mode APCI was carried out using a modified GC-APCI II ion source (Bruker Daltonics, Bremen, Germany) with a corona needle current of 3000 μA. The sample was transported by a high nebulizer gas stream of 5 L/min to suppress contamination signals of the ion source. Dry gas flow was set to 3 L/min. The performance of the instrumentation was checked each day by measuring polystyrene (Sigma-Aldrich) as a standard.[34,45]

Temperature-resolved mass spectra were recorded using a 7 T Fourier transform ion cyclotron resonance mass spectrometer (APEX Qe, Bruker Daltonics, Bremen, Germany). Spectra were acquired with a 2 s transient (4 Megaword), resulting in a mass resolution of 260 000 @m/z 400. To enhance the signal-to-noise ratio, 10 microscans were acquired, resulting in one mass spectrum every 20 s. Data processing was carried out using Bruker DataAnalysis 5.1 for precalibration of the average mass spectra and subsequent export of the line spectra. Data were further processed with the self-written program CERES, which is based on MATLAB scripting (MATLAB 2019b). Blank correction was carried out on the mass list level before sum formula calculation to avoid misassignments of contaminants. Each single spectrum was individually recalibrated on internal homologues series. Normalization was carried out by the weight portion of the sample subjected to the thermobalance to compensate for the variations by different sample amounts. Time-resolved features were then traced with a feature error border of 5 ppm and a sum formula error of 1 ppm. Sum formulae were assigned using the following restrictions: #C 4−100, #H 4−200, #N 0−1, #O 0−2, #S 0−3, H/C ratio 0.4−2.4, ring and double-bond equivalent (DBE) 0−40, and m/z range 100−1000.

RESULTS AND DISCUSSION

Athabasca asphaltenes, highly enriched in archipelago-type compounds, and Wyoming asphaltenes, highly enriched in island-type structural motifs, were fractionated by extrography.[51] In the present study, the whole asphaltenes were compared to their solubility fractions distinctly differing in compositional space,[51] which are, in particular, the acetone-soluble fraction, the heptane-/toluene-soluble (Hep/Tol) fraction, and the tetrahydrofuran-/toluene-/methanol-soluble (THF/Tol/MeOH) fraction. Table 1 presents the total recovery of the fractionation procedure, as well as the weight percent of the investigated fractions. Wyoming asphaltenes were enriched in the acetone fraction with 35.4 wt %, while Athabasca asphaltenes revealed 24.1 wt %. The latter value is in accordance with Peng et al., who revealed that 20 wt % Athabasca asphaltenes were extractable with acetone.[55] The Hep/Tol fraction comprised 23.2 wt % for Athabasca and 36 wt % for Wyoming asphaltenes. Athabasca asphaltenes are enriched in compounds extracted by Tol/THF/MeOH (43.5 wt %) compared to 25.1 wt % for the Wyoming asphaltenes.

Table 1. Overview of the Total Recovery and Weight Percent of the Fractions Obtained by Extrography Fractionation as well as Percentage of Mass Loss and the Maximum Mass Loss Temperature Revealed by Thermal Gravimetry

	Athabasca			
	whole sample	acetone	Hep/Tol	THF/Tol/MeOH
weight % fraction		24.1	23.2	43.5
total recovery after extrography (%)			90.8	
max. mass loss temp. (°C)	430	420	430	420
dividing temperature between desorption and pyrolysis (°C)		315	-	330
mass loss desorption phase (%)		16	0	36
fraction proportion weighted mass loss (desorption phase) (%)			19.5	
mass loss pyrolysis phase (%)	50	45	62	27
fraction proportion weighted mass loss (pyrolysis phase) (%)			37	
total mass loss (%)	50	61	62	63
fraction proportion weighted total mass loss (%)			56.5	
	Wyoming			
	whole sample	acetone	Hep/Tol	THF/Tol/MeOH
weight % fraction		35.4	36.0	25.1
total recovery after extrography (%)			96.5	
max. mass loss temp. (°C)	435	450	450	440
dividing temperature between desorption and pyrolysis (°C)		330	330	300
mass loss desorption phase (%)		12	19	21
fraction proportion weighted mass loss (desorption phase) (%)			16.4	
mass loss pyrolysis phase (%)	22	31	17	20
fraction proportion weighted mass loss (pyrolysis phase) (%)			22.1	
total mass loss (%)	22	43	36	41
fraction proportion weighted total mass loss (%)			38.5	

The pyrolysis of asphaltenes was applied for decades to investigate their structural building blocks and to reduce their chemical complexity hardly accessible comprehensively by any analytical technique.[11,33,37,38,40,56] Figure 1 depicts the three main pathways asphaltenes undergo during evolved gas analysis. (1) Low-molecular-weight compounds, typically present in the maltene fraction, were shown to evaporate intact.[34] With regard to the investigated asphaltenes, primarily occluded maltenes' release should occur in the desorption phase.[34] The structures presented in Figure 1 are based on exemplary sum formula assignments and DBE values of asphaltene compounds investigated in this study as well as structural moieties described in the literature for crude oils and asphaltenes.[12,36,40,55,57,58] A slight contribution to the mass loss below 300−350 °C can also be caused by the evolution of small gases, such as hydrogen sulfide, carbon dioxide, and carbon monoxide, which derive from the decomposition of thermally labile chemical functionalities. (2) From 300 to 350

https://dx.doi.org/10.1021/acs.energyfuels.0c03751
Energy Fuels 2021, 35, 3808−3824

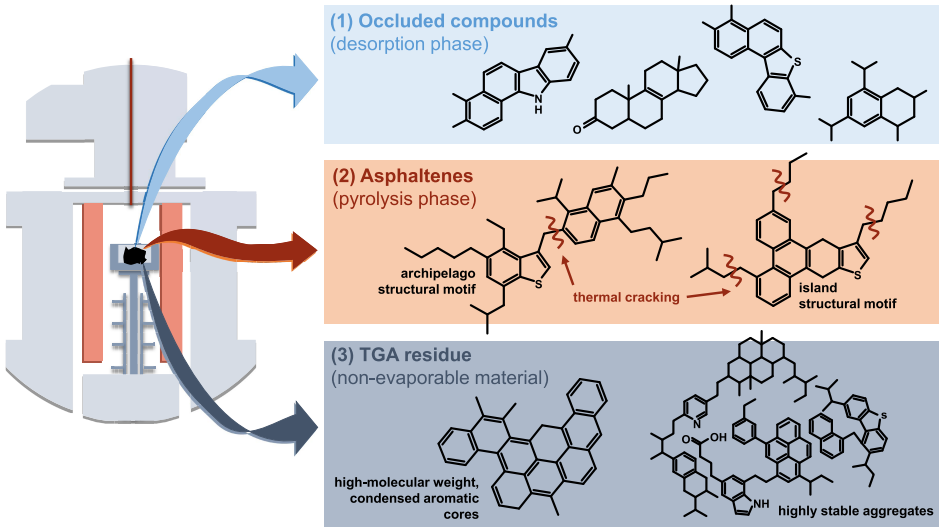

Figure 1. Schematic representation of the primary evolved gas analysis pathways. (1) Low-molecular-weight compounds are evaporated intact in the desorption phase. (2) During the pyrolysis phase, asphaltenes are cracked, releasing smaller building blocks. (3) Extremely high aromatic compounds tend to form coke, which remains as thermal gravimetric analysis (TGA) residue.

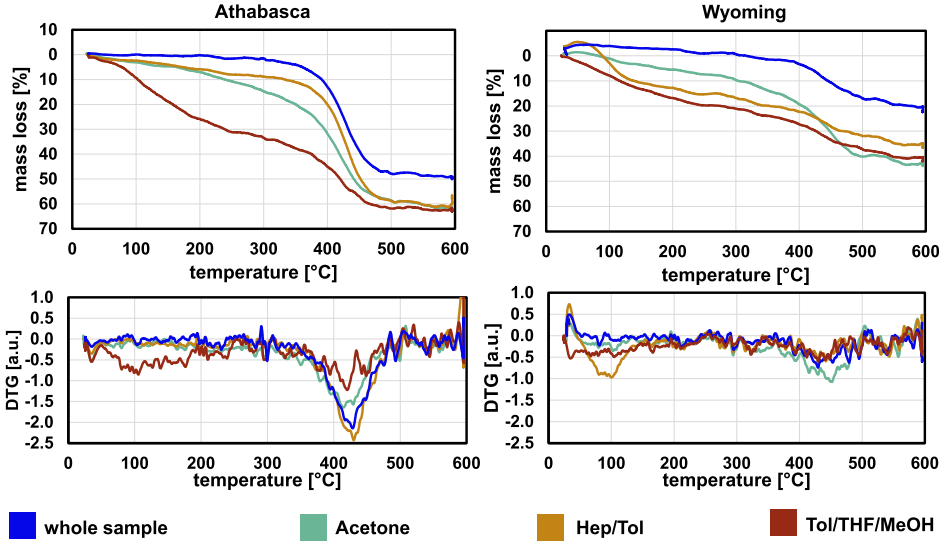

Figure 2. Mass loss diagrams and corresponding DTG signals during TGA of Athabasca and Wyoming asphaltenes and their respective extrography fractions.

°C, pyrolysis of asphaltenes starts by thermal decomposition of C−C and C−S bonds,[59] releasing smaller structural elements in the gas phase. Archipelago-type structures are preferably cracked at alkyl linkers between two smaller core structures.[10,35] Island-type structural motifs, however, are known to cleave off alkyl side chains during thermal treatment,[35,60−62] resulting in lowly alkylated, highly aromatic cores clustering at the aromatic limit[63−65] as well as aliphatic compounds. If the aromatic core of island-type asphaltenes is still evaporable, it is detected during the pyrolysis phase; otherwise, (3) extremely highly aromatic cores (high boiling point) tend to form coke and remain as residue.[35,60,61] Furthermore, highly stable aggregates may survive high temperatures during the pyrolysis phase and form coke instead of thermally decomposing into smaller fragments.[66]

Thermal gravimetric analysis (TGA) was frequently used for asphaltenes to determine mass loss, coke yield, and the maximum mass loss temperature in the literature.[34,45,56,67] By applying a thermobalance, mass loss can be traced with increasing temperature in real time, resulting in a mass loss diagram; however, the differential thermogravimetric (DTG) signal reveals the mass loss rate. Figure 2 shows the mass loss and DTG diagrams of the studied Athabasca and Wyoming asphaltenes and their fractions. Both unfractionated asphaltenes reveal a considerable mass loss between 300 and 500 °C. Friesen et al. already reported for Athabasca asphaltenes that all pyrolyzable material is decomposed below 525 °C,[68] while Huang et al. found that thermal decomposition occurred primarily between 350 and 450 °C for Florida asphaltenes.[69]

In contrast to the whole asphaltenes, the polarity fractions revealed a mass loss below 300 °C, indicating the release of enriched occluded material later discussed in detail. This result is consistent with the supramolecular assembly model for aggregation of asphaltenes introduced by Gray et al.[66] The model implies the occlusion of maltene compounds by, e.g., acid−base interactions, hydrogen bonding, or metal coordina-

https://dx.doi.org/10.1021/acs.energyfuels.0c03751
Energy Fuels 2021, 35, 3808−3824

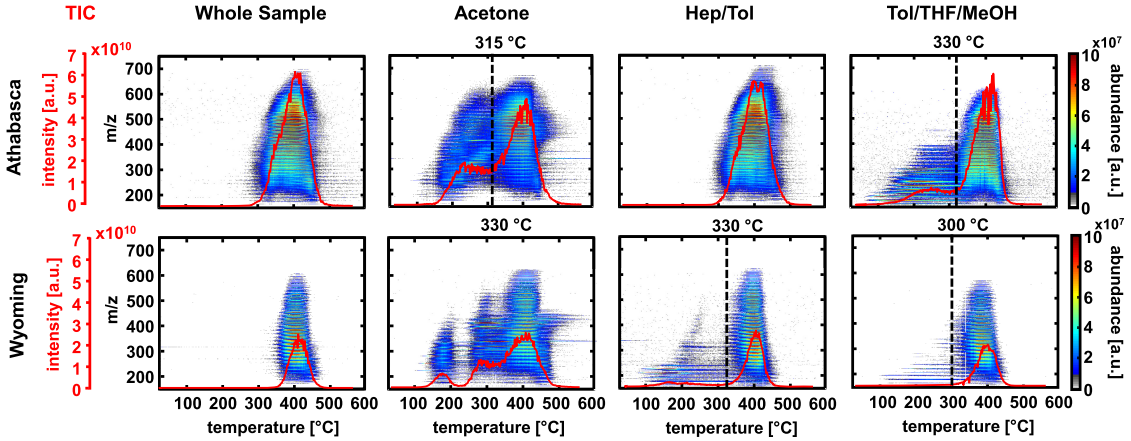

Figure 3. Survey view of the temperature-resolved mass spectra of Athabasca and Wyoming whole asphaltenes and their fractions. The TIC is overlaid in red. Fractions, which revealed occluded material during the desorption phase, are separated at the minimum between desorption and pyrolysis phase.

tion, in addition to the well-known $\pi-\pi$ stacking.[66,70] We hypothesize that during extrography, aggregates are dispersed, allowing the release of smaller occluded materials at lower temperatures. Strikingly, Athabasca asphaltenes revealed for all samples substantially higher mass losses of 50−63% than Wyoming asphaltenes with 22−43%. The difference implies that Wyoming asphaltenes are enriched in components that form nondistillable residues during thermal treatment, such as coke precursors, nonevaporable organic species, compounds with slow pyrolysis rates, or inorganic materials.[34,71,72] It is known that asphaltenes from different geological origins yield different amounts of coke/TGA residue,[32−34,73] and various pyrolysis conditions result in the wide range of residue yields of 35−75% reported in the literature.[37] The TGA residues for Athabasca asphaltenes (47−50%) and Wyoming asphaltenes (57−78%) obtained in this study are consistent with values revealed in earlier studies. Rueda-Velásquez et al. and Karimi et al. reported 46−47% coke yield for Athabasca asphaltenes,[32,33] whereas Juyal et al. reported 69% yield for Wyoming asphaltenes.[72] Concerning the DTG diagrams, Athabasca asphaltenes showed a lower temperature for the maximum weight loss from 420 to 430 °C than Wyoming asphaltenes from 435 to 450 °C. Slightly higher values for the maximum weight loss temperature are found in earlier studies on other asphaltenes, such as Maya asphaltenes (478 °C),[56] Cold Lake bitumen asphaltenes (480 °C)[56] as well as asphaltenes from Garzan (468 °C) and Raman (458 °C) crude oils.[67] Although Maya and Cold Lake bitumen asphaltenes are known for high concentrations of archipelago structural motifs, the reported maximum weight loss temperatures are slightly higher. However, besides the different geological origin of the asphaltenes, the heating rate of the TGA is different compared to the present study (10 vs 5 K/min), which could explain the observed variations. Regarding the different extrographic fractions investigated in this study, both asphaltenes exhibited a higher TGA residue for the whole sample. Without fractionation, Athabasca asphaltenes yield 50% residue, whereas all fractions revealed approximately 40% residue formation. Similar results can be observed for Wyoming asphaltenes, where 78% residue is formed for the whole sample, approximately 60% for the acetone as well as Tol/THF/MeOH fraction, and 64% for the Hep/Tol fraction. It might be expected that the average mass loss of the measured solubility fractions equals the mass loss of the whole asphaltene. However, all investigated fractions revealed a higher mass loss than unfractionated asphaltenes. Therefore, the weighted total mass loss based on the individual fraction proportions as well as the corresponding contributions of the desorption and pyrolysis phase were calculated. For the weighted mass loss, the proportions of the fractions were multiplied with their respective mass loss and summed up, allowing for comparison to the whole sample. The calculated values are summarized in Table 1. For Athabasca asphaltenes, the weighted total mass loss of 56.5% is comparable to the total mass loss of the whole asphaltene of 50% observed during the pyrolysis phase only. Approximately 19.5% of the weighted mass loss corresponds to the desorption phase (occluded material) and 37% corresponds to the pyrolysis phase (pyrolysis products of asphaltenes). For Wyoming asphaltenes, the weighted mass loss accounts for 38.5%, with 16.4% and 22.1% for desorption and pyrolysis phase, respectively. As a result, both asphaltenes show a proportion of material evaporated below 300 °C after the extrography process. Especially for Wyoming asphaltenes, the residue amount could be reduced by enhancing the total mass loss. These findings could support cooperative aggregation of asphaltenes from different solubility fractions forming highly stable aggregates, which are stable at high temperatures and which tend to occur during the pyrolysis phase or even form coke rather than to volatalize. Gray and coworkers demonstrated that model compounds can produce aggregates by $\pi-\pi$ stacking, which are thermally stable above 300 °C and show thermal degradation above 440 °C by coke formation.[74] Furthermore, highly polarizable compounds irreversibly bonding to the silica gel during the fractionation process could additionally be associated with the higher coke residue of the whole asphaltene samples.

A fraction of the gas mixture evolved during TG measurements was investigated online by APCI-FT-ICR MS. The temperature-resolved mass spectra given in Figure 3 provide an overview of the covered mass and temperature range. The total ion chromatogram (TIC) is overlaid in red. Comparison of the whole asphaltenes and their respective solvent fractions reveal remarkably different chemical profiles. As expected for the comparatively steep mass decrease of the TG curve of the whole asphaltenes, Athabasca and Wyoming asphaltenes reveal exclusively mass spectrometric response between 300 and 500

https://dx.doi.org/10.1021/acs.energyfuels.0c03751
Energy Fuels 2021, 35, 3808−3824

°C, with m/z up to 700 for Athabasca and m/z up to 600 for Wyoming asphaltenes. In earlier studies,[34,45] we showed that purified asphaltenes exhibit TG and MS signals exclusively between 300 and 550 °C, when high-molecular-weight structures are thermally cracked under pyrolysis conditions. Compounds desorbed intact below approximately 300 °C were regarded as occluded maltenes, coprecipitated within asphaltene aggregates.[34] Small contributions to the mass loss below 300 °C may be also caused by the evaporation of small gases, such as hydrogen sulfide, carbon dioxide, and carbon monoxide. For most of the solubility fractions, desorbable species also occur during 100−300 °C and were not detected in the whole asphaltenes before. For Athabasca and Wyoming asphaltenes, the acetone fraction reveals the highest content of occluded material, indicating an enrichment of coprecipitated maltenes in this fraction. Athabasca asphaltenes show one apex during the desorption phase with a maximum m/z of 650, which starts at 100 °C and overlaps with the pyrolysis phase. Wyoming asphaltenes reveal two maxima for the desorption phase, the first at 150−230 °C with a mass range between m/z 150 and 450 and the second starting at 250 °C and overlapping with the pyrolysis phase ranging from m/z 200 to 550. It is important to point out that the initial extraction with acetone also aims to extract coprecipitated material that remained after heptane-washing in the standard preparation methods for asphaltene samples.[75] The Hep/Tol fraction of Athabasca asphaltenes covers a similar temperature and mass range as the whole sample. In contrast, Wyoming asphaltenes exhibit a low-abundant pattern during the desorption phase between 100 and 330 °C. The Tol/THF/MeOH fraction shows, for both asphaltenes, the occluded material desorbed at elevated temperature and that overlaps with the actual pyrolysis phase. For this fraction, Athabasca asphaltenes reveal a higher content of occluded compounds, with most of the material having m/z values below 400, whereas Wyoming asphaltenes exhibit few compounds with m/z mostly below 300 in this fraction.

To investigate the chemical differences of the asphaltene building blocks and the occluded maltenes occurring in the different fractions, the time-resolved mass spectra were separated into two individual phases. As separation temperature, the minimum of the TIC signal between the desorbed compounds and the pyrolysis fragments is chosen. The separation temperatures slightly differ between the samples and are given for the individual fractions above the dashed lines in Figure 3. The slight shift in the separation temperature suggests variations in structural and chemical functionalities between the molecules involved in the desorption and pyrolysis processes. As pointed out, the molecular profiles of both phases overlap to a certain extent, making this approach partially artificial. Nevertheless, the desorption phase, up to 300−330 °C, is dominated by the occluded material, whereas the pyrolysis phase is dominated by the asphaltene building blocks.

Occluded Compounds. Due to extensive washing,[51,53] the whole asphaltene samples do not reveal appreciable amounts of occluded compounds during thermal analysis.[34,45] Nonetheless, after the extrography fractionation, occluded compounds can be successfully exposed and seem to be enriched in several fractions, especially in the acetone fraction. The temperature profile of the TIC in Figure 3 of the desorbed compounds indicates that those species are real occluded compounds and not low-molecular-weight asphaltenes. The TIC clearly exhibits a bimodal behavior although both phases reveal an overlap for most of the fractions. If the species occurring in the desorption phase were low-molecular-weight asphaltenes, they should reveal a continuous increase in boiling point in congruence with the Boduszynski continuum model,[43,76−78] instead of the present prelocated distribution.

Figure 4 a depicts the compound class distribution of the desorption phase for all samples of Athabasca and Wyoming

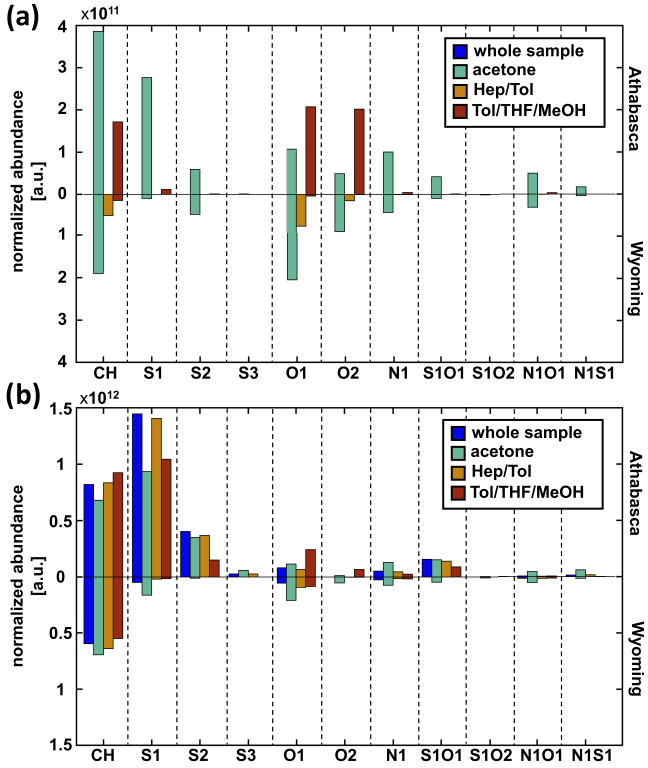

Figure 4. Overview of the normalized abundance of the compound classes of the whole asphaltenes and their solvent fractions for (a) the desorption phase and (b) the pyrolysis phase. The data is normalized to the sample amount subjected to the thermobalance.

asphaltenes. Athabasca asphaltenes showed intact desorbed occluded maltenes for the acetone and Tol/THF/MeOH fractions, while Wyoming asphaltenes revealed a desorbable material for the acetone, Hep/Tol, and Tol/THF/MeOH fractions. The acetone fraction exhibited for both asphaltenes the largest chemical diversity, covering the CH, S1, S2, O1, O2, N1, S1O1, N1O1, and N1S1 classes. The Athabasca asphaltene acetone fraction additionally reveals a small content of occluded S3-class species. In comparison to the acetone fraction of the Wyoming asphaltenes, the occluded material of Athabasca asphaltenes is enriched in the CH class and sulfur-containing classes, such as S1−S3, S1O1, and N1S1, whereas occluded compounds of Wyoming asphaltenes predominantly reveal CH, O1, and O2 class species. The Wyoming Hep/Tol fraction also reveals occluded compounds mainly of CH, O1, and O2 class species. Athabasca asphaltenes reveal a much higher content of occluded material in the Tol/THF/MeOH fraction than Wyoming asphaltenes. In this fraction, Athabasca asphaltenes are enriched in the CH, O1, and O2 classes, indicating a higher content of polarizable functional groups, likely capable of interacting through hydrogen bonding with the actual asphaltene molecules. The few compounds

https://dx.doi.org/10.1021/acs.energyfuels.0c03751
Energy Fuels 2021, 35, 3808−3824

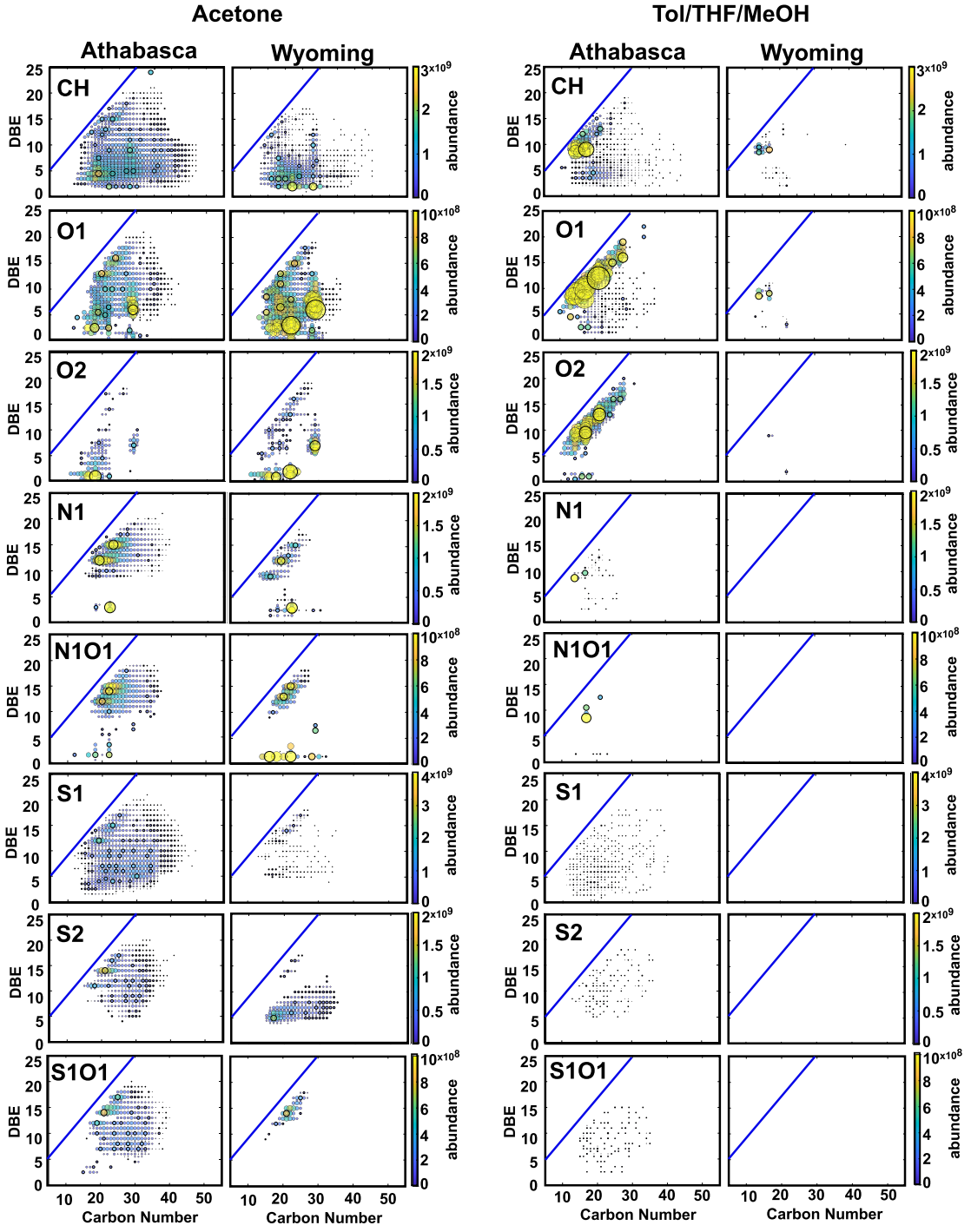

Figure 5. DBE vs #C plots summed over the desorption range of the TG-APCI-FT-ICR MS spectra for the acetone and Tol/THF/MeOH fractions of different compound classes occluded by Athabasca and Wyoming asphaltenes. The blue line indicates the planar aromatic limit.

occurring in the desorption phase of the Wyoming asphaltene Tol/THF/MeOH fraction predominantly belong to the CH class.

The occluded compounds vary not only in their absolute abundance between the two asphaltenes but also in their compositional space. DBE vs #C diagrams represent the compositional space by number of rings plus double bonds (DBE, *y*-axis) and molecular weight (carbon number, *x*-axis) and are presented in Figure 5 for the most abundant compound classes for the acetone and Tol/THF/MeOH fractions. In Figure S1, the DBE vs #C plots are presented without the intensity-based size-coding to avoid the overlapping of the most abundant species. DBE vs #C diagrams for the Hep/Tol fraction of Wyoming asphaltenes are given in Figures S2 and S3 in the Supporting Information. The blue line integrated in the DBE vs #C plots illustrates the planar aromatic hydrocarbon limit (PAH limit). The planar aromatic hydrocarbon limit is defined by the most compact PAHs, which are fused peri-condensed compounds.[63−65] These species are the most thermodynamically and kinetically stable.[64,79]

https://dx.doi.org/10.1021/acs.energyfuels.0c03751
Energy Fuels 2021, 35, 3808−3824

Acetone Fraction. Acetone is known to extract occluded maltenes, low-molecular-weight asphaltenes, and asphaltene compounds with dominant island structures.[47,49,55,80] For both investigated asphaltenes, the extraction with acetone yielded the highest content of occluded material, which features the broadest compositional space in terms of compound class distribution and compositional space. For most of the compound classes, Athabasca asphaltenes reveal a higher alkylation, whereas the Wyoming occluded material exhibited mostly species clustering at the planar aromatic hydrocarbon limit (alkyl deficient). The CH class of Athabasca asphaltene occluded material reveals species with DBEs up to 20 and carbon numbers up to 47, with a maximum between 15 and 30 carbon atoms and DBEs below 10 as well as several, less alkylated compounds clustering at the aromatic limit. Wyoming asphaltenes reveal a lower proportion of CH-class compounds with an overall smaller covered compositional space with species up to 40 carbon atoms and a maximum between 15 and 25 and DBEs below 8. The O1 class is less abundant in Athabasca occluded compounds compared to Wyoming asphaltenes but cover a slightly broader compositional space. Similar abundance trends are observed for the O2 class. Occluded nitrogen-containing species are abundant for the acetone fraction for both asphaltenes. Athabasca asphaltenes reveal predominantly N1-class species with DBEs between 9 and 20 and carbon numbers up to 40. Prominent species with DBEs 12 and 15 could tentatively be attributed to carbazoles[58,81] with one to two additional, condensed aromatic rings. Occluded Wyoming N1 compounds are comparatively less alkylated, with DBE 9, 12, and 15 as the most prominent. N1O1 compounds reveal rather analogical behaviors for both asphaltenes.

Athabasca asphaltenes are known to have a high concentration of sulfur-containing species.[36] The S1 class of occluded Athabasca compounds covers a broad compositional space with carbon numbers between 12 and 45 and DBEs up to 20. For this class, the abundance of low-DBE compounds with high alkylation and species clustering at the aromatic limit is quite equally distributed. Similar trends are observed for the S2 and S1O1 classes with slightly lower maximum carbon numbers. Wyoming asphaltenes only reveal small amounts of occluded sulfur components. The S1 and S1O1 classes exhibit mostly highly aromatic species with low alkylation. Interestingly and atypical compared to other compound classes, the S2 class only shows a small proportion of high aromatic species, whereas most of the compounds occur with DBEs between 4−11 and 15−35 carbon atoms. This comparatively high abundance of low-DBE, highly alkylated compounds suggests that the occluded S2 species in Wyoming asphaltenes are more likely composed of two smaller, sulfur-containing cores linked by alkyl bridges rather than one highly aromatic core structure.

Hep/Tol Fraction. In the FT-ICR MS spectra, solely Wyoming asphaltenes exhibit occluded materials in the Hep/Tol fraction, although there is a slight mass loss below 300 °C for Athabasca asphaltenes as well. The observed mass decrease without a mass spectrometric signal can presumably be explained by the release of small gases, such as hydrogen sulfide, carbon dioxide, or methane,[38] which cannot be ionized by APCI. Furthermore, the detection of very-low-molecular-weight molecules with an m/z value below 100 is limited by the ion transmission of the FT-ICR MS system. Because of the high sulfur content of Athabasca asphaltenes and the relatively low polar solubility fraction, it is likely that the release of hydrogen sulfide or small sulfides[41] is responsible for the mass loss during the desorption phase without the mass spectrometric detection of occluded material. Wyoming asphaltenes, however, revealed the CH, O1, and O2 classes as the most prominent compound classes. In Figures S2 and S3, the DBE vs #C diagram of the CH class reveals species covering 15−40 carbon atoms with DBEs up to 15. Compounds with 10−20 carbons and DBEs up to 5−10 occur with a higher abundance. The covered compositional space of the O1 class is much smaller. Occluded O1-class compounds are predominantly clustered at the PAH limit, with species consisting of 10−20 carbon atoms and abundant DBEs between 5 and 10. The O2 class reveals only a few compounds occurring in the maximum range of the O1 class.

Tol/THF/MeOH Fraction. With respect to the mass loss diagrams in Figure 2 and the temperature-resolved mass spectra in Figure 3, it turns out that the Tol/THF/MeOH fraction shows for both asphaltenes a higher mass loss than the acetone fraction for temperatures below 300 °C but a substantially lower mass spectrometric response. Due to the relatively high polarity of the Tol/THF/MeOH fraction, this effect might be explained by the thermal decomposition of carbonyl and carboxyl functionalities. The decomposition process might cause the release of carbon monoxide or carbon dioxide, both of which cannot be ionized by APCI. If the polar functionalities are cleaved off from alkane- or naphthenic structures, the nonpolar remaining compounds cannot or only hardly be ionized with low response factors by the applied ionization technique, which may also contribute to the discrepancy observed between mass loss and the mass spectrometric signal.

In contrast to the previously discussed fractions, the Tol/THF/MeOH fraction of Athabasca asphaltenes reveals a high content of occluded compounds clustering at the PAH limit with DBEs up to 20 and only a few compounds with low DBEs and high alkylation. However, Wyoming asphaltenes exhibit only minor amounts of occluded compounds, mostly represented in the CH and O1 classes with a narrow range of 13−17 carbon atoms and DBE values between 8 and 10. Since asphaltenes eluted with Tol/THF/MeOH were shown to be enriched in archipelago-type structural motifs,[49] this result further supports Gray's hypothesis that archipelago-type asphaltenes can easier occlude maltenes than island-type molecules.[66] In an earlier study, Athabasca asphaltenes were shown to be enriched in archipelago-type structures compared to Wyoming asphaltenes, which may explain the higher abundance of occluded material found in the Athabasca samples.

The CH class of Athabasca asphaltene occluded compounds contained highly abundant, aromatic species with 13−22 carbon atoms and DBE values of 8−15 as well as comparatively lower abundant compounds with 13−35 carbon atoms and DBEs below 7. The O1 and particularly the O2 class are shifted toward the planar aromatic limit. Although Wyoming asphaltenes are enriched in oxygen-containing occluded material (acetone and Hep/Tol fractions), they only exhibit small amounts of Ox species in the Tol/THF/MeOH fraction, whereas Athabasca asphaltenes are enriched in O1- and O2-class species that concentrate in the most polarizable extrography fraction (Tol/THF/MeOH). Since the oxygen species occur in different solvent fractions with different polarities, it can be assumed that oxygen species present in the acetone and Hep/Tol fractions are less polarizable than species

https://dx.doi.org/10.1021/acs.energyfuels.0c03751
Energy Fuels 2021, 35, 3808−3824

eluted by Tol/THF/MeOH. Thus, in the less polar fractions, oxygen might be contained as ketone functionalities should be enriched, whereas highly polarizable fractions may contain hydroxyl and carboxylic acid functionalities, capable of hydrogen-bonding interactions with the silanol groups of the silica gel or polarizable asphaltene species. Strausz et al. summarized detailed investigations on occluded materials obtained in the Soxhlet-extracted acetone fraction of Athabasca asphaltenes.[58] A series of ketones, carboxylic acids, and minor amounts of alcohols were found by different analytical techniques[58] although the results are not completely comparable to the present study due to the lacking adsorption of the asphaltenes on silica gel prior to solvent treatment. In a more recent study, occluded compounds on asphaltenes were obtained by Soxhlet extraction with *n*-heptane and investigated by APPI-FT-ICR MS.[53] The highest polar fraction revealed CH, O1, S1, and N1 class species with low-molecular-weight compounds shifted toward the aromatic limit as well. It was concluded that these compounds strongly interact with the asphaltene molecules by hydrogen bonding, acid−base interactions, or π-stacking due to the high aromaticity.[53] Although the present asphaltenes underwent the same extensive washing process as the samples in the mentioned study, a small amount of strongly bonded compounds remains occluded within the asphaltene macrostructures and is released during the heating process of the thermobalance, indicating that not all occluded material can be removed by washing with *n*-heptane.

Several works indicate that coprecipitates such as resins or aromatics are mostly composed of islandlike structural motifs.[44,47] Regarding the observations within the different compound classes in this study, it can be concluded that occluded compounds can cover two different compositional spaces. The first region contains species with high aromaticity and short alkylation, while the other region is composed of compounds with lower DBE and higher carbon numbers. It depends on the compound class and the solubility fraction as well as the asphaltene origin, how pronounced the different regions are. For the CH, O1, S1, S2, and S1O1 classes, both compositional regions are covered, while the N1 and N1O1 classes only exhibit highly aromatic species. This bimodal distribution was also previously observed for midpolar fractions of occluded CH-, O1-, and S1-class compounds of a Colombian asphaltene.[53] Highly aromatic compounds with short alkylation were classified as "asphaltene-like" structures, while low-DBE compounds were classified as "maltene-like" structures, forming a compositional gap between both regions.[53] Furthermore, the results indicate that aggregation has large influences on the release of the occluded material also at very high temperatures. In the whole asphaltene samples, the occluded compounds may be prevented from TG desorption by cooperative aggregation, which can explain the absence of species in the desorption phase. The acetone fraction was shown to have a low aggregation potential,[49] which prevents occlusion in aggregates and is consistent with the high amount of detected occluded material. These findings strengthen the idea of cooperative aggregation between asphaltene molecules of different fractions, which are partially separated during the extrography procedure.

Pyrolysis Phase of the Whole Asphaltenes and Their Extrography Fractions. The fractionation of crude-oil-derived material has been shown to provide great advantages in its molecular characterization by FT-ICR MS by increasing the number of attributed sum formulae and differentiating between chemical functionalities as well as structural motifs.[82−85] Although temperature-resolved evolved gas analysis already enables a thermal separation of the asphaltene matrix, additional fractionation increases the number of assigned compounds, which is depicted as Venn diagrams in Figure 6. For Wyoming asphaltenes, a 2-fold increase of

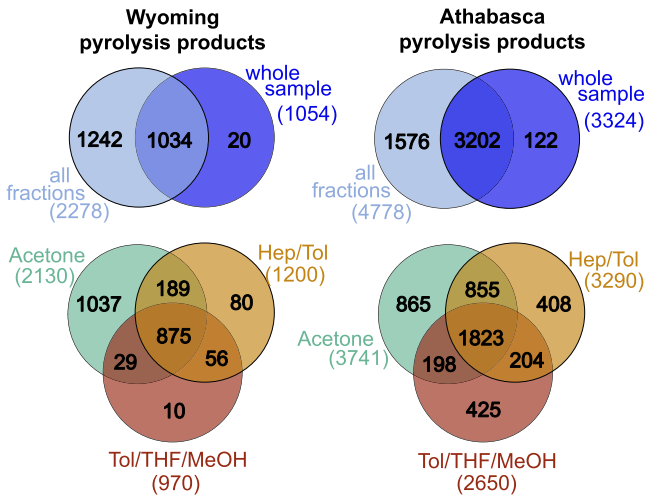

Figure 6. Venn diagrams of assigned sum formulae of Wyoming and Athabasca asphaltene pyrolysis products as well as their solubility fractions.

assigned molecular formulas is observed, whereas Athabasca asphaltenes reveal approximately a 1.5-fold increase of detected sum formulae. Regarding the extrographic fractions, the acetone fraction exhibited the highest amount of attributed sum formulae in both asphaltenes. This result further indicates the influence of aggregation on the thermal decomposition behavior of asphaltenes. Because of the low aggregation tendency of asphaltenes eluted with acetone, the non-aggregated asphaltenes could decompose more easily, which leads to the release of smaller, evaporable pyrolysis products. For fractions with a high aggregation tendency, such as Tol/THF/MeOH, aggregates may prevent thermal decomposition and lead to coke formation instead.

In Figure 4b, the compound class distribution of the pyrolysis phase is presented. While the occluded material mostly covers specific compound classes only, the asphaltene pyrolysis products were found for all main compound classes. Athabasca asphaltene pyrolysis products cover the CH, S1, S2, S3, O1, O2, N1, S1O1, S1O2, N1O1, and N1S1 classes, which together account for 97−100% of the total assigned absolute abundance. Pyrolysis products of Wyoming asphaltenes reveal mainly the same compound classes except for the S2 and S3 classes, which together account for 99−100% of the total assigned absolute abundance. At first glance, the revealed compound classes exhibit unsuspected low complexity compared to direct infusion studies. However, the detected compounds are pyrolysis fragments of the asphaltenes showing probably reduced complexity because of pyrolytic cracking. If a poly-heteroatomic multicore asphaltene, which contains heteroatoms in several cores, is cracked, the remaining fragments will occur in different compound classes. Regarding single-core asphaltenes, poly-heteroatomic asphaltenes most likely cleave of alky side chains, leaving the core intact. In Figure 7, examples are presented for both types of asphaltenes.

https://dx.doi.org/10.1021/acs.energyfuels.0c03751
Energy Fuels 2021, 35, 3808−3824

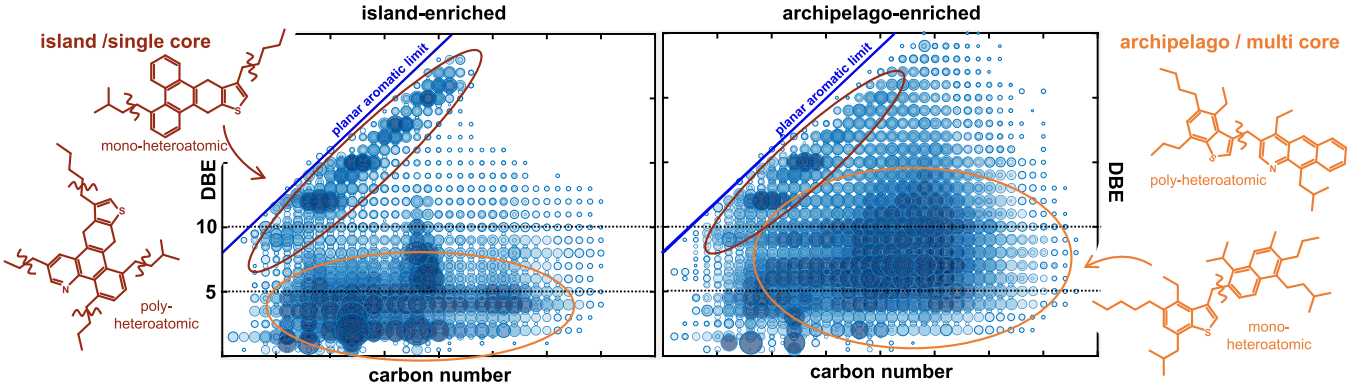

Figure 7. Exemplary DBE vs #C diagram of the pyrolysis phase with all compound classes overlaid for island-enriched (Wyoming) and archipelago-enriched (Athabasca) asphaltenes. The shown molecules serve only as exemplary asphaltene structures. Two distinct regions are revealed, in which pyrolysis fragments are observed with high abundance. The first region (red) is observed for species clustering at the aromatic limit with comparatively high DBE values. Those pyrolysis fragments are most likely derived from islandlike asphaltenes, which cleaved of alkyl side chains or smaller pendant groups by leaving the highly aromatic core intact. The second region (orange) is observed at lower DBE values and higher carbon numbers. Those pyrolysis fragments most likely are derived from the cleavage of multicore/archipelago-type asphaltenes and small pendant groups from island structural motifs. Multicores are preferentially cracked at their bridges, which reduces the DBE value. Nonetheless, the alkyl side chains of the aforementioned archipelago-type structures are mostly preserved; therefore, those pyrolysis fragments occur at comparatively high carbon numbers.

On the left side, a possible structure for a single-core asphaltene of the N1S1 class is shown. After thermal cracking and cleavage of the side chains, the aromatic core remains in the N1S1 class. In contrast, a possible multicore asphaltene of the N1S1 class shown on the right side is likely to be cracked into two smaller core structures. If the heteroatoms are present in different cores, the fragments will occur in the N1 class and S1 class, with respect to the presented example. This type of thermal degradation might give rise to mono-heteroatomic compound classes. Similar trends were previously observed by investigating the compositional changes of asphaltenes during thermal cracking and hydroconversion by direct infusion APPI-FT-ICR MS.[35] The maltene fraction obtained by cracking was shown to contain only nine major compound classes, while the parent asphaltenes consisted of 21 classes.[35]

By investigating the DBE vs #C diagrams of asphaltenes decomposed during pyrolysis, two distinct regions of highly abundant thermal fragments become apparent. Figure 7 provides exemplary DBE vs #C diagrams for the pyrolysis phase of the acetone fraction of an island-enriched asphaltene (Wyoming) and an archipelago-enriched asphaltene (Athabasca). All compound classes are overlaid. The first region (red) is observed for thermal fragments with high DBE values and low carbon numbers indicating low alkylation, which cluster near the planar aromatic hydrocarbon limit. Those pyrolysis fragments are most likely derived from the thermal decomposition of island-type/single-core asphaltenes cleaving off alkyl side chains as well as small pendant groups and leaving the aromatic cores intact.[35,60−62] Island-enriched asphaltenes are more pronounced in this region than archipelago-enriched asphaltenes. The second region (orange) is observed for lower DBE values and comparatively high carbon numbers. Island-enriched asphaltenes are in this region enriched in pyrolysis fragments with DBE values below 5. This finding indicates that the observed fragments derive from alkyl side chains, which might contain small naphthenic or phenylic pendant groups, cleaved off during pyrolysis. Archipelago-enriched asphaltenes reveal only a minor amount of exceptionally low DBE-species. However, those asphaltenes exhibit high abundant signal for thermal fragments with DBE values between 4 and 15. These species are likely to be derived from archipelago/multicore asphaltenes, which are preferentially cracked at linkers bridging the aromatic cores, which decreases the DBE values.[10,35,59] Due to preserving the alkyl side chains, those thermal decomposition products occur at comparatively high carbon numbers. However, also side reactions between radicals formed during pyrolysis could generate species with high carbon numbers.

In Figure 8, DBE vs #C plots of the four most abundant compound classes in both asphaltenes, namely, the CH, O1, S1, and N1 classes, are presented. Corresponding DBE vs #C plots without the intensity-based size-coding are shown in Figure S5. The covered compositional space of the shown classes is comparable to the maltene fraction of thermal upgrading products of Colombian asphaltenes investigated by DI-APPI-FT-ICR MS.[35] Especially, the CH class with highly abundant low-DBE compounds and the N class with species abundant for DBE 9 and higher reveal great similarity between both studies. Regarding the whole asphaltenes compared to their extrography fractions, the samples differ in the covered compositional space. For Athabasca asphaltenes, the compositional space of the whole asphaltene sample is quite similar to the Hep/Tol fraction, while Wyoming asphaltenes revealed similarity to the Hep/Tol and Tol/THF/MeOH fractions. These findings differ from results revealed by direct infusion FT-ICR MS, where the acetone fraction was shown to mainly equal the whole asphaltene sample.[49] Acetone was found to elute compounds with a high monomeric ion yield due to its sufficient solvation ability of small, pericondensed aromatic hydrocarbons,[49] such as highly occluded material and low-molecular-weight, islandlike asphaltenes.[14,80,86,87] These findings led to the assumption that mass spectrometry, assisted by atmospheric pressure photoionization (APPI), reflects mainly the components with the highest monomer ion yield.[49] For the TG-FT-ICR MS coupling applied in this study, comparatively strong matrix effects caused by the acetone fraction were not observed because TG provides a separation of the compounds by their thermal behavior, which partially overcomes matrix effects observed for direct infusion techniques.

https://dx.doi.org/10.1021/acs.energyfuels.0c03751
Energy Fuels 2021, 35, 3808−3824

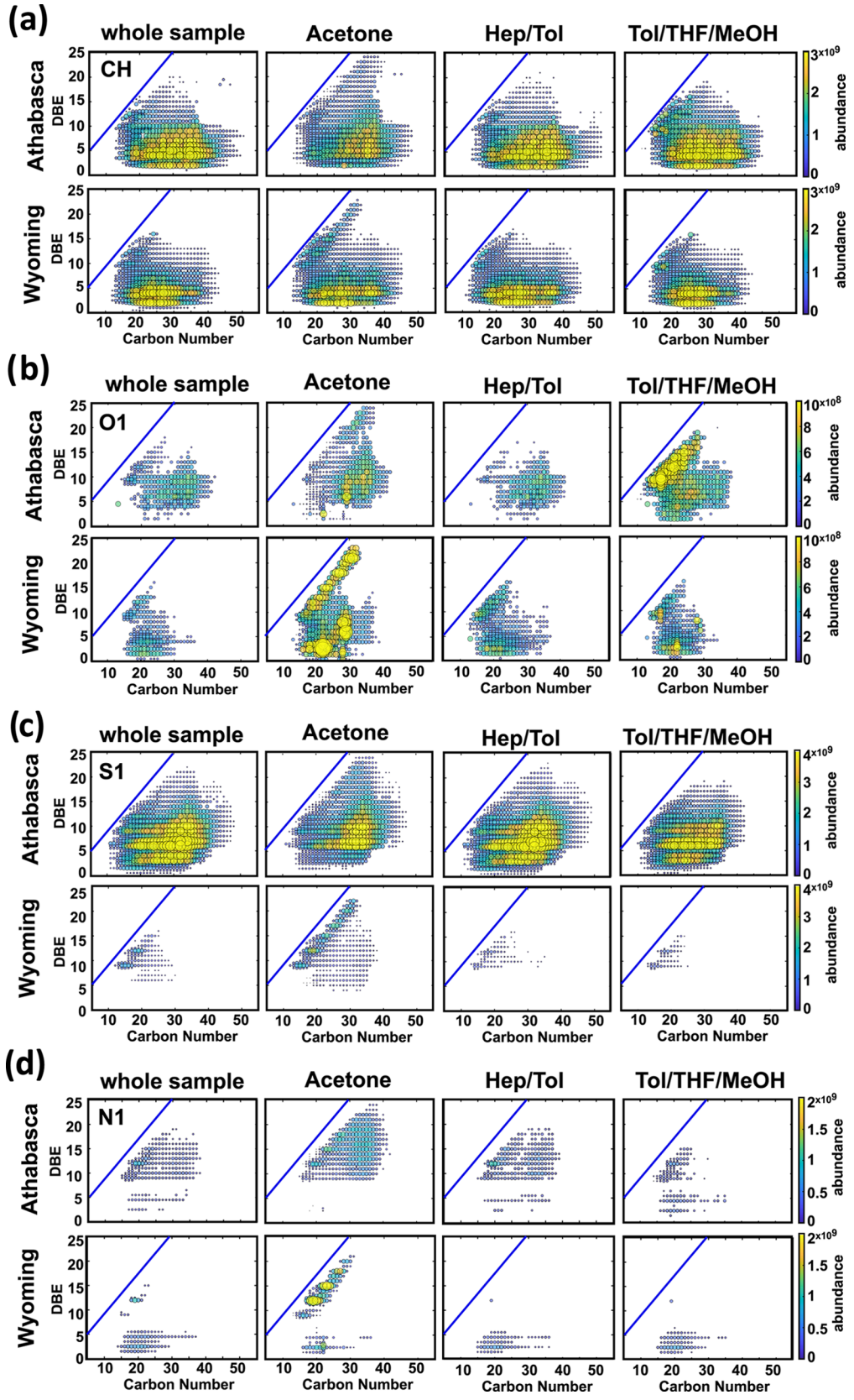

Figure 8. DBE vs #C diagrams of the pyrolysis fragments of Athabasca and Wyoming whole asphaltenes and their fractions measured by TG-APCI-FT-ICR MS: (a) CH class, (b) O1 class, (c) S1 class, and (d) N1 class. The blue line indicates the planar aromatic limit.

As depicted in Figure 8a, whole Athabasca asphaltenes reveal pyrolysis fragments with DBEs up to 20 and carbon numbers up to 50 for the CH class, with species below DBE 10 as the most prevalent. A substantial amount of highly abundant compounds was also observed below the aromatic boundary of DBE 4. These compounds most probably correspond to

https://dx.doi.org/10.1021/acs.energyfuels.0c03751
Energy Fuels 2021, 35, 3808−3824

alkenes produced by thermal cracking of alkyl side chains[88] as well as building blocks containing naphthenic structural elements.[26,33,56] Wyoming whole asphaltenes revealed a lower maximum DBE of 16 and carbon numbers up to 45, with high amounts of non- or low-aromatic CH-class pyrolysis fragments detected. The non- or low-aromatic fragments most probably are derived from the cleavage of small naphthenic or even aromatic pendant groups or alkyl side chains, forming alkenes by hydrogen abstraction[88] due to the thermal cracking process. Considering that Wyoming asphaltenes are enriched in island structural motifs compared to Athabasca asphaltenes, the higher abundance of species with DBE 4 or lower can be explained by the aforementioned thermal degradation reaction. This difference between both asphaltenes in the CH class is observed for all fractions. Furthermore, at first glance, the higher maximum DBE of the CH class observed for species clustering at the aromatic limit in whole Athabasca asphaltenes and all fractions compared to the Wyoming asphaltene equivalents contradicts the fact that Wyoming asphaltenes are enriched in highly aromatic, island-type structures. However, due to the high TGA residue of Wyoming asphaltenes, whose composition was not accessed in this study, it can be assumed that these asphaltenes contain high amounts of compounds with large aromatic, islandlike cores serving as coke precursors. Athabasca asphaltenes, however, seem to contain smaller island-type structures, which are still evaporable after cleaving off the alkyl side chains during the pyrolysis process.

The acetone fraction differs the most from the other fractions, revealing a bimodal distribution of island- and archipelago-type pyrolysis products. Comparable to that, McKenna et al. observed a bimodal distribution by distillation of high petroleum boiling cuts, which was suggested to be derived from thermal cracking of archipelago-type compounds and the detection of island-type structures.[10] The acetone fraction exhibits for both asphaltenes the highest detected DBE values for pyrolysis products. For the CH class, pyrolysis fragments with up to 25 for Athabasca asphaltenes and up to 23 for Wyoming asphaltenes are observed. Nonetheless, Athabasca asphaltenes revealed the highest abundance for building blocks with DBE below 15 and 15−45 carbon atoms, whereas Wyoming asphaltenes are enriched in highly aromatic building blocks (DBE 10−23) clustering at the aromatic limit. The comparatively high amount of highly aromatic species can be explained by the property of acetone to extract asphaltene compounds with a single-core structure, which exhibit a weaker aggregation tendency.[49,86,87] Recently, it was shown that the dominance of island and archipelago structural motifs depends not only on the geological origin of asphaltenes but also on the molecular weight.[51] Lower m/z values and, therefore, low-molecular-weight asphaltenes were found to be enriched in island structural motifs, whereas high m/z values revealed both motif types.[51] As Wyoming asphaltenes contain high amounts of islandlike structures, also low-molecular-weight asphaltenes seem to be enriched in compounds with highly aromatic, condensed cores. Besides the acetone fraction, also the Tol/THF/MeOH fraction reveals differences in the whole sample. Compared to the other fractions, low-DBE CH compounds revealed lower alkylation for both asphaltenes.

Not only the CH class exhibits differences between the whole asphaltenes and their fractions, heteroatom-containing compound classes differ in their compositional space as well. Figure 8b shows DBE vs #C diagrams of the O1 class. In both whole asphaltenes, only minor amounts of oxygen-containing components are detected in the pyrolysis phase. During thermal decomposition, highly polarizable oxygen-containing functionalities could be cleaved off, and more thermally stable oxygen compounds, such as ketones, are mostly detected. For Athabasca asphaltenes, the O1 class is enriched in the acetone and Tol/THF/MeOH fractions, while Wyoming asphaltenes only exhibit higher amounts of oxygen-containing compounds in the acetone fraction. As already revealed for the CH class, both asphaltenes showed in the acetone fraction a distinct bimodal distribution of islandlike and archipelago-like pyrolysis fragments. Highly aromatic pyrolysis products, clustering at the aromatic limit, were detected with DBE values between 10 and 25, while species with higher alkylation, with up to 35−40 carbon atoms, reached DBEs not higher than 15. Specifically, Wyoming asphaltenes revealed a high enrichment in islandlike O1-class compounds; also, higher alkylated species with lower DBEs exhibit a second maximum in absolute abundance. For Athabasca asphaltenes, highly aromatic O1-class fragments are less pronounced in the acetone fraction. However, as observed for occluded materials, highly aromatic species with DBEs between 12 and 20 are enriched in the Tol/THF/MeOH fraction, indicating a higher polarity of the oxygen-containing functionalities compared to those occurring in the acetone fraction. This observation is supported by Frakman et al., who revealed less polar ketones, such as fluorenones (DBE 9) and benzofluorenones (DBE 12), in high quantities in the acetone fraction of Athabasca asphaltenes.[80] Moreover, Nascimento et al. reported a high content of polar functionalities, such as basic nitrogen, carboxylic groups, or ketones, in THF-eluted fractions,[25] supporting the findings for the highly aromatic Athabasca pyrolysis products. Besides, in the THF/MeOH fraction of South American medium asphaltenes and the Petrophase-2017 asphaltene, a high O/C ratio was revealed by APPI-FT-ICR MS, as reported by Rodgers et al.[49] The authors demonstrated that direct infusion experiments on the same asphaltene samples revealed an enrichment of highly aromatic oxygen-containing compounds for Wyoming asphaltenes.[51] With the TG-FT-ICR MS approach, these species were not accessible, although they should have been ionized by APCI. Thus, we hypothesize that these highly polarizable and aromatic compounds remained in the residue during the heating process. It is likely that these compounds undergo thermal decomposition reactions by cleaving of the oxygen-containing chemical functionalities. However, the aromatic core structures seem to be not evaporable, since there is no increase in highly aromatic CH-class compounds, which indicates the formation of coke instead.

Compared to Wyoming asphaltenes, sulfur-containing compounds are more pronounced in Athabasca building blocks, which is demonstrated by the high absolute abundance (Figure 4) and number of assigned sum formulae (Figure S4) of the S1−S3 classes as well as the S1O1 class. In contrast to the occluded compounds of Athabasca asphaltenes, where sulfur species were highly enriched in the acetone fraction, sulfur-containing pyrolysis products were detected with higher absolute abundance in the whole asphaltene and in the Hep/Tol fraction. At the molecular level, differences in the prevalence of structural motifs are observed for both asphaltenes. In the whole sample, S1-class pyrolysis products of Athabasca asphaltenes cover a broad compositional space with up to DBE 22 and 48 carbon atoms. Predominant structural motives feature an archipelago-type character due to

https://dx.doi.org/10.1021/acs.energyfuels.0c03751
Energy Fuels 2021, 35, 3808−3824

DBE values below 12 and high absolute abundance for carbon numbers between 20 and 40. Wyoming asphaltenes only exhibited a limited compositional space of species with higher abundance between DBE 9 and 15 and short alkylation. For the Wyoming asphaltenes, especially building blocks with DBE 9 and 12 are prevalent, which can tentatively be attributed to dibenzothiophenes and benzonaphthothiophenes.[32,36,56] In the acetone fraction, S1-class pyrolysis fragments revealed higher DBE values with DBEs up to 25 for Athabasca asphaltenes and up to 23 for Wyoming asphaltenes. In this fraction, Wyoming asphaltenes are clearly enriched in highly aromatic structures, whereas Athabasca asphaltenes are shifted to lower DBEs with higher alkylation. Remarkably, Athabasca asphaltenes eluted with acetone show only low abundance for S1 compounds with DBEs less than 6 (tentatively benzothiophenes[77]), which is different from all other samples. The Tol/THF/MeOH fraction shows, as already revealed for the CH class, shorter alkylation, which is most probably an effect of the highly polar extraction solvent mixture.

The N1 class of the pyrolyzed asphaltenes in Figure 8d reveals similar main features as previously discussed for the other compound classes. Athabasca asphaltenes exhibited for all fractions predominantly N1-class species with DBEs greater than 10. In the acetone fraction, a bimodal behavior of island- and archipelago-related structures is observed, which is quite balanced between both structural motifs. For this fraction, Wyoming asphaltenes stand in strong contrast to the Athabasca sample. Except for some low-abundant pyrolysis products with small DBEs, Wyoming asphaltenes only exhibit highly aromatic, islandlike structural motifs clustering at the aromatic limit. Other fractions and the whole asphaltene sample mostly exhibit non- to low-aromatic pyrolysis products with DBEs less than 6. This dominant difference between the acetone fraction of Athabasca and Wyoming asphaltenes with regard to the structural motifs is observed for the S1O1, N1O1, and N1S1 classes as well, for which the DBE vs #C diagrams are given in the Supporting Information in Figures S6 and S7, respectively.

The bimodal behavior of island-type and archipelago-type asphaltenes, which was predominant in the acetone fraction for TG-FT-ICR MS, is comparable to observations made by IRMPD-APPI-FT-ICR MS in the literature.[47,49,51] IRMPD fragmentation is based on the uptake of IR photons by vibration states (thermal activation) of gas-phase ions in a high vacuum leading to their fragmentation.[89] To a certain extent, IRMPD can be compared to the thermal cracking that occurs during evolved gas analysis, where molecules are thermally decomposed in the liquid/solid phase under atmospheric pressure with potential molecular interactions. However, it is interesting to note that both techniques provide consistent molecular profiles for asphaltene samples composed of island and archipelago motifs. It was shown for IRMPD that island-type structural motifs cleave off their side chains, which results in similar DBE values but a reduction in carbon number shifting the fragments toward the planar aromatic limit.[47,49] Archipelago-type asphaltenes exhibited an apparent decrease in DBE and carbon number in comparison to the precursor ions in IRMPD.[47,49] In this study, we revealed that thermal analysis provides results consistent with bulk thermal decomposition, since island-enriched samples yield a higher amount of coke/highly aromatic core structures, whereas archipelago-type asphaltenes yield maltenes/low-DBE pyrolysis products. Archipelago-type structural motifs were characterized by low DBE values and a broad carbon number distribution. This result differs from IRMPD, where archipelago fragments are also fragmented down to their core structures because the thermal decomposition under atmospheric pressure enables collisional cooling, preserving the alkyl chains. On the contrary, island-type structures showed highly dealkylated, highly aromatic pyrolysis fragments clustering at the planar aromatic limit and revealed a higher coke formation tendency. Therefore, TG-FT-ICR MS provides an additional technique to investigate the predominant structures in asphaltenes by combining the amount of TGA residue and thermal cracking fragments.

CONCLUSIONS

In this study, two asphaltenes, one enriched in island-type structural motifs (Wyoming asphaltenes) and one in archipelago-type structural motifs (Athabasca asphaltenes), as well as their extrography fractions were investigated by TG-APCI-FT-ICR MS. During desorption up to a temperature of ca. 300 °C, the occluded material was desorbed intact, whereas during the pyrolysis process, thermal fragments of the asphaltenes were detected. The following main conclusions could be revealed by analyzing the thermal decomposition products of the different asphaltenes.

(1) Island-enriched asphaltenes yield higher coke residues than archipelago-enriched asphaltenes.

(2) Whole asphaltenes were found to yield higher amounts of TGA residue than their solubility fractions, which is assumed to be caused by highly polar compounds not eluted during the fractionation process as well as cooperative aggregation between asphaltene molecules of different polarities.

(3) Although the asphaltenes were extensively washed, a highly occluded material was revealed particularly in the acetone and Tol/THF/MeOH fractions, indicating partial separation of cooperative aggregates.

(4) A bimodal behavior was revealed for most of the compound classes of the pyrolysis fragments, representing the presence of archipelago- and island-type structural motifs in both asphaltenes. The bimodal distribution was the most prevalent in the acetone fraction. Especially for the O1 class of Athabasca bitumen, the prevalent structural motif depended on the solubility fraction.

(5) Pyrolysis products with high DBE and short alkylation are likely to originate from island-type asphaltenes, whereas pyrolysis products with low DBE values and high carbon numbers may derive from archipelago-type asphaltenes.

TG-API-FT-ICR MS was shown to successfully address the structural motif debate of asphaltenes. By combining the mass loss information with the molecular fingerprint in terms of characteristic areas in DBE vs #C diagrams for island- and archipelago-type motifs, comparable characteristic shifts could be revealed as shown for DI-IRMPD-FT-ICR MS. Therefore, TG-FT-ICR MS provides a corresponding molecular resolving approach, which cannot be achieved by microscopic, spectroscopic, or even low-resolution pyrolysis techniques. Future studies will focus on the extremely polarizable, irreversibly bonded asphaltene material during extrography fractionation with TG-FT-ICR MS.

https://dx.doi.org/10.1021/acs.energyfuels.0c03751
Energy Fuels 2021, 35, 3808−3824

■ ASSOCIATED CONTENT

Supporting Information

The Supporting Information is available free of charge at https://pubs.acs.org/doi/10.1021/acs.energyfuels.0c03751.

DBE vs #C plots for the desorption range of the acetone and Tol/THF/MeOH fractions with abundance color-coding; DBE vs #C plots for the Hep/Tol fraction occluded compounds with and without abundance size-coding; number of assigned sum formulae of the individual compound classes of the whole asphaltene and its fractions; DBE vs #C plots for the pyrolysis range of the whole asphaltene and its fractions with abundance color-coding; DBE vs #C plots for the pyrolysis range of selected compound classes of the acetone fraction with and without abundance size-coding (PDF)

■ AUTHOR INFORMATION

Corresponding Author

Christopher P. Rüger − *Joint Mass Spectrometry Centre (JMSC)/Chair of Analytical Chemistry, University of Rostock, 18059 Rostock, Germany; Department Life, Light & Matter (LLM), University of Rostock, 18051 Rostock, Germany;* orcid.org/0000-0001-9634-9239; Email: christopher.rueger@uni-rostock.de

Authors

Anika Neumann − *Joint Mass Spectrometry Centre (JMSC)/Chair of Analytical Chemistry, University of Rostock, 18059 Rostock, Germany; Department Life, Light & Matter (LLM), University of Rostock, 18051 Rostock, Germany;* orcid.org/0000-0001-7256-3716

Martha Liliana Chacón-Patiño − *National High Magnetic Field Laboratory and Florida State University, Tallahassee, Florida 32310, United States;* orcid.org/0000-0002-7273-5343

Ryan P. Rodgers − *National High Magnetic Field Laboratory and Florida State University, Tallahassee, Florida 32310, United States;* orcid.org/0000-0003-1302-2850

Ralf Zimmermann − *Joint Mass Spectrometry Centre (JMSC)/Chair of Analytical Chemistry, University of Rostock, 18059 Rostock, Germany; Department Life, Light & Matter (LLM), University of Rostock, 18051 Rostock, Germany; Joint Mass Spectrometry Centre (JMSC)/Helmholtz Zentrum München, Comprehensive Molecular Analytics, 85764 Neuherberg, Germany*

Complete contact information is available at: https://pubs.acs.org/10.1021/acs.energyfuels.0c03751

Notes

The authors declare no competing financial interest.

■ ACKNOWLEDGMENTS

A portion of the work presented herein was performed at the National High Magnetic Field Laboratory ICR User Facility, which is supported by the National Science Foundation Division of Chemistry through Cooperative agreement DMR-1644779, and the State of Florida. Funding by the Horizon 2020 program for the EU FT-ICR MS project (European Network of Fourier-Transform Ion-Cyclotron-Resonance Mass Spectrometry Centers, Grant agreement ID: 731077) is gratefully acknowledged. The authors thank the German Research Foundation (DFG) for funding of the Bruker FT-ICR MS (INST 264/56).

■ REFERENCES

(1) Adams, J. J. Asphaltene Adsorption, a Literature Review. *Energy Fuels* **2014**, *28*, 2831−2856.

(2) Akbarzadeh, K.; Hammami, A.; Kharrat, A.; Zhang, D.; Allenson, S.; Creek, J.; Kabir, S.; Jamaluddin, A. J.; Marshall, A. G.; Rodgers, R. P.; Mullins, O. C.; Solbakken, T. Asphaltenes—Problematic but Rich in Potential. *Oilfield Rev.* **2007**, 22−43.

(3) Buckley, J. S. Asphaltene Deposition. *Energy Fuels* **2012**, *26*, 4086−4090.

(4) Hammami, A.; Ratulowski, J. Precipitation and Deposition of Asphaltenes in Production Systems: A Flow Assurance Overview. In *Asphaltenes, Heavy Oils and Petroleomics*; Mullins, O. C., Ed.; Springer, 2007; pp 617−660.

(5) Moulijn, J. A.; van Diepen, A. E.; Kapteijn, F. Catalyst deactivation: is it predictable? *Appl. Catal., A* **2001**, *212*, 3−16.

(6) Palacio Lozano, D. C.; Thomas, M. J.; Jones, H. E.; Barrow, M. P. Petroleomics: Tools, Challenges, and Developments. *Annu. Rev. Anal. Chem.* **2020**, *13*, 405−430.

(7) Schuler, B.; Meyer, G.; Peña, D.; Mullins, O. C.; Gross, L. Unraveling the Molecular Structures of Asphaltenes by Atomic Force Microscopy. *J. Am. Chem. Soc.* **2015**, *137*, 9870−9876.

(8) Schuler, B.; Fatayer, S.; Meyer, G.; Rogel, E.; Moir, M.; Zhang, Y.; Harper, M. R.; Pomerantz, A. E.; Bake, K. D.; Witt, M.; Peña, D.; Kushnerick, J. D.; Mullins, O. C.; Ovalles, C.; van den Berg, F. G. A.; Gross, L. Heavy Oil Based Mixtures of Different Origins and Treatments Studied by Atomic Force Microscopy. *Energy Fuels* **2017**, *31*, 6856−6861.

(9) Panda, S. K.; Andersson, J. T.; Schrader, W. Characterization of supercomplex crude oil mixtures: what is really in there? *Angew. Chem., Int. Ed.* **2009**, *48*, 1788−1791.

(10) McKenna, A. M.; Chacón-Patiño, M. L.; Weisbrod, C. R.; Blakney, G. T.; Rodgers, R. P. Molecular-Level Characterization of Asphaltenes Isolated from Distillation Cuts. *Energy Fuels* **2019**, *33*, 2018−2029.

(11) Calemma, V.; Rausa, R.; D'Anton, P.; Montanari, L. Characterization of Asphaltenes Molecular Structure. *Energy Fuels* **1998**, *12*, 422−428.

(12) Payzant, J. D.; Lown, E. M.; Strausz, O. P. Structural units of Athabasca asphaltene: the aromatics with a linear carbon framework. *Energy Fuels* **1991**, *5*, 445−453.

(13) McKenna, A. M.; Donald, L. J.; Fitzsimmons, J. E.; Juyal, P.; Spicer, V.; Standing, K. G.; Marshall, A. G.; Rodgers, R. P. Heavy Petroleum Composition. 3. Asphaltene Aggregation. *Energy Fuels* **2013**, *27*, 1246−1256.

(14) Putman, J. C.; Moulian, R.; Barrère-Mangote, C.; Rodgers, R. P.; Bouyssiere, B.; Giusti, P.; Marshall, A. G. Probing Aggregation Tendencies in Asphaltenes by Gel Permeation Chromatography. Part 1: Online Inductively Coupled Plasma Mass Spectrometry and Offline Fourier Transform Ion Cyclotron Resonance Mass Spectrometry. *Energy Fuels* **2020**, *34*, 8308−8315.

(15) Pinkston, D. S.; Duan, P.; Gallardo, V. A.; Habicht, S. C.; Tan, X.; Qian, K.; Gray, M.; Müllen, K.; Kenttämaa, H. I. Analysis of Asphaltenes and Asphaltene Model Compounds by Laser-Induced Acoustic Desorption/Fourier Transform Ion Cyclotron Resonance Mass Spectrometry. *Energy Fuels* **2009**, *23*, 5564−5570.

(16) Pomerantz, A. E.; Hammond, M. R.; Morrow, A. L.; Mullins, O. C.; Zare, R. N. Two-step laser mass spectrometry of asphaltenes. *J. Am. Chem. Soc.* **2008**, *130*, 7216−7217.

(17) Pomerantz, A. E.; Hammond, M. R.; Morrow, A. L.; Mullins, O. C.; Zare, R. N. Asphaltene Molecular-Mass Distribution Determined by Two-Step Laser Mass Spectrometry †. *Energy Fuels* **2009**, *23*, 1162−1168.

(18) Groenzin, H.; Mullins, O. C. Molecular Size and Structure of Asphaltenes from Various Sources. *Energy Fuels* **2000**, *14*, 677−684.

(19) Hurt, M. R.; Borton, D. J.; Choi, H. J.; Kenttämaa, H. I. Comparison of the Structures of Molecules in Coal and Petroleum

Asphaltenes by Using Mass Spectrometry. *Energy Fuels* **2013**, *27*, 3653−3658.
(20) Yen, T. F.; Erdman, J. G.; Pollack, S. S. Investigation of the Structure of Petroleum Asphaltenes by X-Ray Diffraction. *Anal. Chem.* **1961**, *33*, 1587−1594.
(21) Mullins, O. C. The Modified Yen Model †. *Energy Fuels* **2010**, *24*, 2179−2207.
(22) Schuler, B.; Zhang, Y.; Collazos, S.; Fatayer, S.; Meyer, G.; Pérez, D.; Guitián, E.; Harper, M. R.; Kushnerick, J. D.; Peña, D.; Gross, L. Characterizing aliphatic moieties in hydrocarbons with atomic force microscopy. *Chem. Sci.* **2017**, *8*, 2315−2320.
(23) Zhang, Y.; Schuler, B.; Fatayer, S.; Gross, L.; Harper, M. R.; Kushnerick, J. D. Understanding the Effects of Sample Preparation on the Chemical Structures of Petroleum Imaged with Noncontact Atomic Force Microscopy. *Ind. Eng. Chem. Res.* **2018**, *57*, 15935−15941.
(24) Chen, P.; Metz, J. N.; Mennito, A. S.; Merchant, S.; Smith, S. E.; Siskin, M.; Rucker, S. P.; Dankworth, D. C.; Kushnerick, J. D.; Yao, N.; Zhang, Y. Petroleum pitch: Exploring a 50-year structure puzzle with real-space molecular imaging. *Carbon* **2020**, *161*, 456−465.
(25) Nascimento, P. T. H.; Santos, A. F.; Yamamoto, C. I.; Tose, L. V.; Barros, E. V.; Gonçalves, G. R.; Freitas, J. C. C.; Vaz, B. G.; Romão, W.; Scheer, A. P. Fractionation of Asphaltene by Adsorption onto Silica and Chemical Characterization by Atmospheric Pressure Photoionization Fourier Transform Ion Cyclotron Resonance Mass Spectrometry, Fourier Transform Infrared Spectroscopy Coupled to Attenuated Total Reflectance, and Proton Nuclear Magnetic Resonance. *Energy Fuels* **2016**, *30*, 5439−5448.
(26) Artok, L.; Su, Y.; Hirose, Y.; Hosokawa, M.; Murata, S.; Nomura, M. Structure and Reactivity of Petroleum-Derived Asphaltene. *Energy Fuels* **1999**, *13*, 287−296.
(27) Sabbah, H.; Morrow, A. L.; Pomerantz, A. E.; Mullins, O. C.; Tan, X.; Gray, M. R.; Azyat, K.; Tykwinski, R. R.; Zare, R. N. Comparing Laser Desorption/Laser Ionization Mass Spectra of Asphaltenes and Model Compounds. *Energy Fuels* **2010**, *24*, 3589−3594.
(28) Sabbah, H.; Morrow, A. L.; Pomerantz, A. E.; Zare, R. N. Evidence for Island Structures as the Dominant Architecture of Asphaltenes. *Energy Fuels* **2011**, *25*, 1597−1604.
(29) Tang, W.; Hurt, M. R.; Sheng, H.; Riedeman, J. S.; Borton, D. J.; Slater, P.; Kenttämaa, H. I. Structural Comparison of Asphaltenes of Different Origins Using Multi-stage Tandem Mass Spectrometry. *Energy Fuels* **2015**, *29*, 1309−1314.
(30) Riedeman, J. S.; Kadasala, N. R.; Wei, A.; Kenttämaa, H. I. Characterization of Asphaltene Deposits by Using Mass Spectrometry and Raman Spectroscopy. *Energy Fuels* **2016**, *30*, 805−809.
(31) Borton, D.; Pinkston, D. S.; Hurt, M. R.; Tan, X.; Azyat, K.; Scherer, A.; Tykwinski, R.; Gray, M.; Qian, K.; Kenttämaa, H. I. Molecular Structures of Asphaltenes Based on the Dissociation Reactions of Their Ions in Mass Spectrometry. *Energy Fuels* **2010**, *24*, 5548−5559.
(32) Rueda-Velásquez, R. I.; Freund, H.; Qian, K.; Olmstead, W. N.; Gray, M. R. Characterization of Asphaltene Building Blocks by Cracking under Favorable Hydrogenation Conditions. *Energy Fuels* **2013**, *27*, 1817−1829.
(33) Karimi, A.; Qian, K.; Olmstead, W. N.; Freund, H.; Yung, C.; Gray, M. R. Quantitative Evidence for Bridged Structures in Asphaltenes by Thin Film Pyrolysis. *Energy Fuels* **2011**, *25*, 3581−3589.
(34) Rüger, C. P.; Neumann, A.; Sklorz, M.; Schwemer, T.; Zimmermann, R. Thermal Analysis Coupled to Ultrahigh Resolution Mass Spectrometry with Collision Induced Dissociation for Complex Petroleum Samples: Heavy Oil Composition and Asphaltene Precipitation Effects. *Energy Fuels* **2017**, *31*, 13144−13158.
(35) Chacón-Patiño, M. L.; Blanco-Tirado, C.; Orrego-Ruiz, J. A.; Gómez-Escudero, A.; Combariza, M. Y. Tracing the Compositional Changes of Asphaltenes after Hydroconversion and Thermal Cracking Processes by High-Resolution Mass Spectrometry. *Energy Fuels* **2015**, *29*, 6330−6341.
(36) Strausz, O. P.; Mojelsky, T. W.; Faraji, F.; Lown, E. M.; Peng, P. Additional Structural Details on Athabasca Asphaltene and Their Ramifications. *Energy Fuels* **1999**, *13*, 207−227.
(37) Gray, M. R. Consistency of Asphaltene Chemical Structures with Pyrolysis and Coking Behavior. *Energy Fuels* **2003**, *17*, 1566−1569.
(38) Savage, P. E.; Klein, M. T.; Kukes, S. G. Asphaltene reaction pathways. 1. Thermolysis. *Ind. Eng. Chem. Process Des. Dev.* **1985**, *24*, 1169−1174.
(39) Savage, P. E.; Klein, M. T.; Kukes, S. G. Asphaltene reaction pathways. 3. Effect of reaction environment. *Energy Fuels* **1988**, *2*, 619−628.
(40) Strausz, O. P.; Mojelsky, T. W.; Lown, E. M. The molecular structure of asphaltene: an unfolding story. *Fuel* **1992**, *71*, 1355−1363.
(41) Strausz, O. P.; Mojelsky, T. W.; Lown, E. M.; Kowalewski, I.; Behar, F. Structural Features of Boscan and Duri Asphaltenes. *Energy Fuels* **1999**, *13*, 228−247.
(42) Marshall, A. G.; Rodgers, R. P. Petroleomics: chemistry of the underworld. *Proc. Natl. Acad. Sci. U.S.A.* **2008**, *105*, 18090−18095.
(43) McKenna, A. M.; Marshall, A. G.; Rodgers, R. P. Heavy Petroleum Composition. 4. Asphaltene Compositional Space. *Energy Fuels* **2013**, *27*, 1257−1267.
(44) Podgorski, D. C.; Corilo, Y. E.; Nyadong, L.; Lobodin, V. V.; Bythell, B. J.; Robbins, W. K.; McKenna, A. M.; Marshall, A. G.; Rodgers, R. P. Heavy Petroleum Composition. 5. Compositional and Structural Continuum of Petroleum Revealed. *Energy Fuels* **2013**, *27*, 1268−1276.
(45) Rüger, C. P.; Grimmer, C.; Sklorz, M.; Neumann, A.; Streibel, T.; Zimmermann, R. Combination of Different Thermal Analysis Methods Coupled to Mass Spectrometry for the Analysis of Asphaltenes and Their Parent Crude Oils: Comprehensive Characterization of the Molecular Pyrolysis Pattern. *Energy Fuels* **2018**, *32*, 2699−2711.
(46) Giraldo-Dávila, D.; Chacón-Patiño, M. L.; McKenna, A. M.; Blanco-Tirado, C.; Combariza, M. Y. Correlations between Molecular Composition and Adsorption, Aggregation, and Emulsifying Behaviors of PetroPhase 2017 Asphaltenes and Their Thin-Layer Chromatography Fractions. *Energy Fuels* **2018**, *32*, 2769−2780.
(47) Chacón-Patiño, M. L.; Rowland, S. M.; Rodgers, R. P. Advances in Asphaltene Petroleomics. Part 1: Asphaltenes Are Composed of Abundant Island and Archipelago Structural Motifs. *Energy Fuels* **2017**, *31*, 13509−13518.
(48) Putman, J. C.; Moulian, R.; Smith, D. F.; Weisbrod, C. R.; Chacón-Patiño, M. L.; Corilo, Y. E.; Blakney, G. T.; Rumancik, L. E.; Barrère-Mangote, C.; Rodgers, R. P.; Giusti, P.; Marshall, A. G.; Bouyssière, B. Probing Aggregation Tendencies in Asphaltenes by Gel Permeation Chromatography. Part 2: Online Detection by Fourier Transform Ion Cyclotron Resonance Mass Spectrometry and Inductively Coupled Plasma Mass Spectrometry. *Energy Fuels* **2020**, 10915.
(49) Chacón-Patiño, M. L.; Rowland, S. M.; Rodgers, R. P. Advances in Asphaltene Petroleomics. Part 2: Selective Separation Method That Reveals Fractions Enriched in Island and Archipelago Structural Motifs by Mass Spectrometry. *Energy Fuels* **2018**, *32*, 314−328.
(50) Rodgers, R. P.; Mapolelo, M. M.; Robbins, W. K.; Chacón-Patiño, M. L.; Putman, J. C.; Niles, S. F.; Rowland, S. M.; Marshall, A. G. Combating selective ionization in the high resolution mass spectral characterization of complex mixtures. *Faraday Discuss.* **2019**, *218*, 29−51.
(51) Chacón-Patiño, M. L.; Rowland, S. M.; Rodgers, R. P. Advances in Asphaltene Petroleomics. Part 3. Dominance of Island or Archipelago Structural Motif Is Sample Dependent. *Energy Fuels* **2018**, *32*, 9106−9120.
(52) Neumann, A.; Käfer, U.; Gröger, T.; Wilharm, T.; Zimmermann, R.; Rüger, C. P. Investigation of Aging Processes in Bitumen at the Molecular Level with High-Resolution Fourier-

https://dx.doi.org/10.1021/acs.energyfuels.0c03751
Energy Fuels 2021, 35, 3808−3824

Transform Ion Cyclotron Mass Spectrometry and Two-Dimensional Gas Chromatography Mass Spectrometry. *Energy Fuels* **2020**, *34*, 10641−10654.
(53) Chacón-Patiño, M. L.; Vesga-Martínez, S. J.; Blanco-Tirado, C.; Orrego-Ruiz, J. A.; Gómez-Escudero, A.; Combariza, M. Y. Exploring Occluded Compounds and Their Interactions with Asphaltene Networks Using High-Resolution Mass Spectrometry. *Energy Fuels* **2016**, *30*, 4550−4561.
(54) Rüger, C. P.; Miersch, T.; Schwemer, T.; Sklorz, M.; Zimmermann, R. Hyphenation of Thermal Analysis to Ultrahigh-Resolution Mass Spectrometry (Fourier Transform Ion Cyclotron Resonance Mass Spectrometry) Using Atmospheric Pressure Chemical Ionization For Studying Composition and Thermal Degradation of Complex Materials. *Anal. Chem.* **2015**, *87*, 6493−6499.
(55) Peng, P.; Morales-Izquierdo, A.; Hogg, A.; Strausz, O. P. Molecular Structure of Athabasca Asphaltene: Sulfide, Ether, and Ester Linkages. *Energy Fuels* **1997**, *11*, 1171−1187.
(56) Douda, J.; Llanos, M. E.; Alvarez, R.; Franco, C. L.; de La Fuente, J. A. M. Pyrolysis applied to the study of a Maya asphaltene. *J. Anal. Appl. Pyrolysis* **2004**, *71*, 601−612.
(57) Qian, K.; Robbins, W. K.; Hughey, C. A.; Cooper, H. J.; Rodgers, R. P.; Marshall, A. G. Resolution and Identification of Elemental Compositions for More than 3000 Crude Acids in Heavy Petroleum by Negative-Ion Microelectrospray High-Field Fourier Transform Ion Cyclotron Resonance Mass Spectrometry. *Energy Fuels* **2001**, *15*, 1505−1511.
(58) Strausz, O. P.; Torres, M.; Lown, E. M.; Safarik, I.; Murgich, J. Equipartitioning of Precipitant Solubles between the Solution Phase and Precipitated Asphaltene in the Precipitation of Asphaltene. *Energy Fuels* **2006**, *20*, 2013−2021.
(59) Zhao, Y.; Gray, M. R.; Chung, K. H. Molar Kinetics and Selectivity in Cracking of Athabasca Asphaltenes. *Energy Fuels* **2001**, *15*, 751−755.
(60) Hauser, A.; AlHumaidan, F.; Al-Rabiah, H.; Halabi, M. A. Study on Thermal Cracking of Kuwaiti Heavy Oil (Vacuum Residue) and Its SARA Fractions by NMR Spectroscopy. *Energy Fuels* **2014**, *28*, 4321−4332.
(61) Chiaberge, S.; Guglielmetti, G.; Montanari, L.; Salvalaggio, M.; Santolini, L.; Spera, S.; Cesti, P. Investigation of Asphaltene Chemical Structural Modification Induced by Thermal Treatments. *Energy Fuels* **2009**, *23*, 4486−4495.
(62) Douda, J.; Alvarez, R.; Navarrete Bolaños, J. Characterization of Maya Asphaltene and Maltene by Means of Pyrolysis Application. *Energy Fuels* **2008**, *22*, 2619−2628.
(63) Cho, Y.; Kim, Y. H.; Kim, S. Planar limit-assisted structural interpretation of saturates/aromatics/resins/asphaltenes fractionated crude oil compounds observed by Fourier transform ion cyclotron resonance mass spectrometry. *Anal. Chem.* **2011**, *83*, 6068−6073.
(64) Hsu, C. S.; Lobodin, V. V.; Rodgers, R. P.; McKenna, A. M.; Marshall, A. G. Compositional Boundaries for Fossil Hydrocarbons. *Energy Fuels* **2011**, *25*, 2174−2178.
(65) Lobodin, V. V.; Marshall, A. G.; Hsu, C. S. Compositional space boundaries for organic compounds. *Anal. Chem.* **2012**, *84*, 3410−3416.
(66) Gray, M. R.; Tykwinski, R. R.; Stryker, J. M.; Tan, X. Supramolecular Assembly Model for Aggregation of Petroleum Asphaltenes. *Energy Fuels* **2011**, *25*, 3125−3134.
(67) Karacan, O.; Kok, M. V. Pyrolysis Analysis of Crude Oils and Their Fractions. *Energy Fuels* **1997**, *11*, 385−391.
(68) Friesen, W. I.; Michaelian, K. H.; Long, Y.; Dabros, T. Effect of Solvent-to-Bitumen Ratio on the Pyrolysis Properties of Precipitated Athabasca Asphaltenes. *Energy Fuels* **2005**, *19*, 1109−1115.
(69) Huang, J. Characterization of Thermally Degraded Asphaltene Fractions Using Gel Permeation Chromatography. *Pet. Sci. Technol.* **2007**, *25*, 1313−1320.
(70) Murgich, J.; Abanero, J. A.; Strausz, O. P. Molecular Recognition in Aggregates Formed by Asphaltene and Resin Molecules from the Athabasca Oil Sand. *Energy Fuels* **1999**, *13*, 278−286.
(71) Murugan, P.; Mahinpey, N.; Mani, T. Thermal cracking and combustion kinetics of asphaltenes derived from Fosterton oil. *Fuel Process. Technol.* **2009**, *90*, 1286−1291.
(72) Juyal, P.; McKenna, A. M.; Fan, T.; Cao, T.; Rueda-Velásquez, R. I.; Fitzsimmons, J. E.; Yen, A.; Rodgers, R. P.; Wang, J.; Buckley, J. S.; Gray, M. R.; Allenson, S. J.; Creek, J. Joint Industrial Case Study for Asphaltene Deposition. *Energy Fuels* **2013**, *27*, 1899−1908.
(73) Nali, M.; Corana, F.; Montanari, L. Pyrolysis/gas chromatography/mass spectrometry in the analysis of asphaltenes. *Rapid Commun. Mass Spectrom.* **1993**, *7*, 684−687.
(74) Rakotondradany, F.; Fenniri, H.; Rahimi, P.; Gawrys, K. L.; Kilpatrick, P. K.; Gray, M. R. Hexabenzocoronene Model Compounds for Asphaltene Fractions: Synthesis & Characterization. *Energy Fuels* **2006**, *20*, 2439−2447.
(75) Liao, Z.; Zhou, H.; Graciaa, A.; Chrostowska, A.; Creux, P.; Geng, A. Adsorption/Occlusion Characteristics of Asphaltenes: Some Implication for Asphaltene Structural Features. *Energy Fuels* **2005**, *19*, 180−186.
(76) Boduszynski, M. M.; McKay, J. F.; Latham, D. R. In *Asphaltenes, Where Are You?*, Association of Asphalt Paving Technologists Proceedings, 1980; pp 123−143.
(77) McKenna, A. M.; Purcell, J. M.; Rodgers, R. P.; Marshall, A. G. Heavy Petroleum Composition. 1. Exhaustive Compositional Analysis of Athabasca Bitumen HVGO Distillates by Fourier Transform Ion Cyclotron Resonance Mass Spectrometry: A Definitive Test of the Boduszynski Model. *Energy Fuels* **2010**, *24*, 2929−2938.
(78) Ovalles, C.; Moir, M. E., Eds; *The Boduszynski Continuum: Contributions to the Understanding of the Molecular Composition of Petroleum*; ACS Symposium Series; American Chemical Society, 2018; Vol. *1282*.
(79) Ruiz-Morales, Y. HOMO−LUMO Gap as an Index of Molecular Size and Structure for Polycyclic Aromatic Hydrocarbons (PAHs) and Asphaltenes: A Theoretical Study. I. *J. Phys. Chem. A* **2002**, *106*, 11283−11308.
(80) Frakman, Z.; Ignasiak, T. M.; Lown, E. M.; Strausz, O. P. Oxygen compounds in Athabasca asphaltene. *Energy Fuels* **1990**, *4*, 263−270.
(81) Cheshkova, T. V.; Sergun, V. P.; Kovalenko, E. Y.; Gerasimova, N. N.; Sagachenko, T. A.; Min, R. S. Resins and Asphaltenes of Light and Heavy Oils: Their Composition and Structure. *Energy Fuels* **2019**, *33*, 7971−7982.
(82) Giraldo-Dávila, D.; Chacón-Patiño, M. L.; Orrego-Ruiz, J. A.; Blanco-Tirado, C.; Combariza, M. Y. Improving compositional space accessibility in (+) APPI FT-ICR mass spectrometric analysis of crude oils by extrography and column chromatography fractionation. *Fuel* **2016**, *185*, 45−58.
(83) Cho, Y.; Na, J.-G.; Nho, N.-S.; Kim, S.; Kim, S. Application of Saturates, Aromatics, Resins, and Asphaltenes Crude Oil Fractionation for Detailed Chemical Characterization of Heavy Crude Oils by Fourier Transform Ion Cyclotron Resonance Mass Spectrometry Equipped with Atmospheric Pressure Photoionization. *Energy Fuels* **2012**, *26*, 2558−2565.
(84) Clingenpeel, A. C.; Rowland, S. M.; Corilo, Y. E.; Zito, P.; Rodgers, R. P. Fractionation of Interfacial Material Reveals a Continuum of Acidic Species That Contribute to Stable Emulsion Formation. *Energy Fuels* **2017**, *31*, 5933−5939.
(85) Gaspar, A.; Zellermann, E.; Lababidi, S.; Reece, J.; Schrader, W. Characterization of Saturates, Aromatics, Resins, and Asphaltenes Heavy Crude Oil Fractions by Atmospheric Pressure Laser Ionization Fourier Transform Ion Cyclotron Resonance Mass Spectrometry. *Energy Fuels* **2012**, *26*, 3481−3487.
(86) Buenrostro-Gonzalez, E.; Andersen, S. I.; Garcia-Martinez, J. A.; Lira-Galeana, C. Solubility/Molecular Structure Relationships of Asphaltenes in Polar and Nonpolar Media. *Energy Fuels* **2002**, *16*, 732−741.

https://dx.doi.org/10.1021/acs.energyfuels.0c03751
Energy Fuels 2021, 35, 3808−3824

(87) Buenrostro-Gonzalez, E.; Groenzin, H.; Lira-Galeana, C.; Mullins, O. C. The Overriding Chemical Principles that Define Asphaltenes. *Energy Fuels* **2001**, *15*, 972−978.
(88) Moldoveanu, S. C. Chapter 7 Pyrolysis of Hydrocarbons. In *Pyrolysis of Organic Molecules with Applications to Health and Environmental Issues*, 1st ed.; Moldoveanu, Ş., Ed.; Techniques and Instrumentation in Analytical Chemistry; Elsevier, 2010; Vol. *28*, pp 131−229.
(89) Brodbelt, J. S. Photodissociation mass spectrometry: new tools for characterization of biological molecules. *Chem. Soc. Rev.* **2014**, *43*, 2757−2783.

https://dx.doi.org/10.1021/acs.energyfuels.0c03751
Energy Fuels 2021, 35, 3808−3824